



HAL
open science

Aurones and derivatives as promising New Delhi metallo- β -lactamase (NDM-1) inhibitors

Jérémy Caburet, Federica Verdirosa, Matis Moretti, Brayon Roulier, Giorgia Simoncelli, Romain Haudecoeur, Somayeh Ghazi, Hélène Jamet, Jean-Denis Docquier, Benjamin Boucherle, et al.

► To cite this version:

Jérémy Caburet, Federica Verdirosa, Matis Moretti, Brayon Roulier, Giorgia Simoncelli, et al.. Aurones and derivatives as promising New Delhi metallo- β -lactamase (NDM-1) inhibitors. *Bioorganic and Medicinal Chemistry Letters*, 2024, 97, pp.117559. 10.1016/j.bmc.2023.117559 . hal-04429770

HAL Id: hal-04429770

<https://hal.science/hal-04429770>

Submitted on 31 Jan 2024

HAL is a multi-disciplinary open access archive for the deposit and dissemination of scientific research documents, whether they are published or not. The documents may come from teaching and research institutions in France or abroad, or from public or private research centers.

L'archive ouverte pluridisciplinaire **HAL**, est destinée au dépôt et à la diffusion de documents scientifiques de niveau recherche, publiés ou non, émanant des établissements d'enseignement et de recherche français ou étrangers, des laboratoires publics ou privés.

Aurones and derivatives as promising New Delhi metallo- β -lactamase (NDM-1) inhibitors

Jérémy Caburet^a, Federica Verdirosa^{b,‡}, Matis Moretti^{a,‡}, Brayan Roulier^a, Giorgia Simoncelli^b, Romain Haudecoeur^a, Somayeh Ghazi^{a,1}, H  l  ne Jamet^c, Jean-Denis Docquier^{b,d}, Benjamin Boucherle^{a, } and Marine Peuchmaur^{a, ,*}

^a Univ. Grenoble Alpes, CNRS, DPM, 38000 Grenoble, France

^b Dipartimento di Biotecnologie Mediche, Universit   degli Studi di Siena, 53100 Siena, Italy

^c Univ. Grenoble Alpes, CNRS, DCM, 38000 Grenoble, France

^d Laboratoire de Bact  riologie Mol  culaire, UR-InBioS, Universit   de Li  ge, 4000 Li  ge, Belgium

*Marine Peuchmaur, Univ. Grenoble Alpes, CNRS, DPM, B  timent E P  le Chimie BP 53, 38000 Grenoble, France; <https://orcid.org/0000-0002-8926-1922>

Phone: +33 4 76 63 52 95; Email: marine.peuchmaur@univ-grenoble-alpes.fr

Keywords: NDM-1, aurone, metallo- β -lactamase, structure-activity relationship

ABSTRACT

Bacterial resistance is undoubtedly one of the main public health concerns especially with the emergence of metallo- β -lactamases (MBLs) able to hydrolytically inactivate β -lactam antibiotics. Currently, there are no inhibitors of MBLs in clinical use to rescue antibiotic action and the New Delhi metallo- β -lactamase-1 (NDM-1) is still considered as one of the most relevant targets for inhibitor development. Following a fragment-based strategy to find new NDM-1 inhibitors, we identified aurone as a promising scaffold. A series of 60 derivatives were then evaluated and two of them were identified as promising inhibitors with K_i values as low as 1.7 and 2.5 μ M. Moreover, these two most active compounds were able to potentiate meropenem in *in vitro* antimicrobial susceptibility assays. The molecular modelling provided insights about their likely interactions with the active site of NDM-1, thus enabling further improvement in the structure of this new inhibitor family.

1. Introduction

Antibiotics have been successfully used for over 80 years to treat bacterial infections, making an invaluable contribution to human medicine and global public health. However, the misuse and overuse of antibiotics, combined with the extraordinary evolutionary capabilities of bacteria led to the emergence and spread of resistant isolates in the clinical setting accounting for over 1.2 M deaths per year worldwide (in 2019) while significantly increasing healthcare costs [1,2]. β -lactam antibiotics were and still are the most widely used antibacterial drugs, and remain a valuable source of recently approved antibacterial therapies, either alone (e.g. cefiderocol) or in combination with β -lactamase

[‡] Both junior investigators equally contributed to the work.

[ ] Both senior investigators equally contributed to the work.

¹ Current affiliation: Wetherill Laboratory of Chemistry, Department of Chemistry, Purdue University, West Lafayette, IN, US.

inhibitors (e. g. ceftazidime-avibactam, meropenem-vaborbactam) (Fig. 1). These combinations include molecules targeting hydrolytic bacterial enzymes representing, especially in Gram-negative opportunistic pathogens, one of the most important mechanisms of resistance to β -lactams, i.e. β -lactamases. These enzymes, which hydrolyze the amide bond of the β -lactam ring to yield an inactive product, can be divided into four classes on the basis of their primary structure, reflecting an important structural and functional heterogeneity. Class A, C and D enzymes are serine- β -lactamases (SBLs) that open the β -lactam ring of antibiotics through a catalytic mechanism involving the transient covalent bonding of the antibiotic to an active-site serine residue. By contrast, class B β -lactamases are zinc-dependent metallo-hydrolases that use one or two divalent zinc cations to activate a nucleophilic water molecule to hydrolyze the substrate. Metallo- β -lactamases (MBLs) can be further divided into three subclasses (B1, B2 and B3) according to the nature and position of zinc ligands and the number of Zn ions in their active site. Among these enzymes, subclass B1 enzymes are currently the most prevalent and clinically significant MBLs.

Clinically-relevant MBLs are characterized by an exceedingly broad substrate profile, which includes the last-resort drugs carbapenems notably used to treat infections caused by multidrug-resistant clinical isolates. MBLs (such as VIM-2 or NDM-1) are increasingly found in the clinical setting (especially in WHO “critical priority” pathogens for antibiotic R&D, namely carbapenem-resistant *Enterobacterales*, *Pseudomonas aeruginosa* and *Acinetobacter baumannii*) and represent a worrisome addition to the already circulating active serine carbapenemases (such as KPC-3 or OXA-48), as combinations with MBL inhibitors are currently unavailable for clinical uses. MBLs therefore represent both a threat to public health and a challenge to medicinal chemists attempting to develop more effective β -lactam-based antibacterials [3–5]. Indeed, the discovery and development of MBL inhibitors, despite intense scientific research, [6–10] appears difficult and has still not yielded approved combinations, although taniborbactam, a pan-spectrum bicyclic boronate inhibitor, developed in association with cefepime (Fig. 1), completed phase 3 clinical trials in 2022 [11]. Xeruborbactam (QPX7728), an orally available inhibitor exploiting a similar scaffold also completed phase 1 clinical trials in combination with the β -lactam QPX2014 [12].

The New Delhi metallo- β -lactamase-1 (NDM-1), first discovered in 2008, [13] is now regarded, together with other 40 clinical variants, as one of the most relevant target for inhibitor development [14]. As a consequence, several studies have been devoted to the design of NDM-1 inhibitors and more than 500 compounds have been characterized to date [15–20]. Since the antibiotic β -lactam ring hydrolysis involves two Zn(II) ions in the active site of NDM-1, most of the reported inhibitors share common properties or structural patterns: they either include chelating moieties (e.g. 1,4,7-triazacyclononane-1,4,7-triacetic acid (NOTA)), mercapto aliphatic acids (e.g. D-captopril) or natural product pedigree (e.g. aspergillomarasmine A (AMA)) (Fig. 1). However, these inhibitors intervene through various mechanisms of action: for instance, while D-captopril binds to the active site, AMA extracts Zn ions from their active site. Other inhibitors, such as ebselen, an organoselenium compound presenting toxicity issues, are known to covalently bind with a cysteine residue at the active site of NDM-1. Finally, considering the paucity of NDM-1 inhibitors amenable to drug development, finding new effective inhibitors allowing to stem threatening resistant antibiotic infections is now of utmost urgency.

Recently, we undertook a fragment-based drug discovery study [21] to identify new scaffolds of NDM-1 inhibitors. This work led us to evaluate the biological activity of some flavonoids available in our laboratory that included fragments previously highlighted by a Saturation Transfer Difference (STD) NMR screening, such as the 2-hydroxyacetophenone (2-HAP) and/or the catechol fragments. As a result, auronones and indanones were identified as promising NDM-1 inhibitors, showing both *in vitro*

inhibitory activity and some level of carbapenem potentiation in whole-cell assays against NDM-producing strains (Fig. 1).

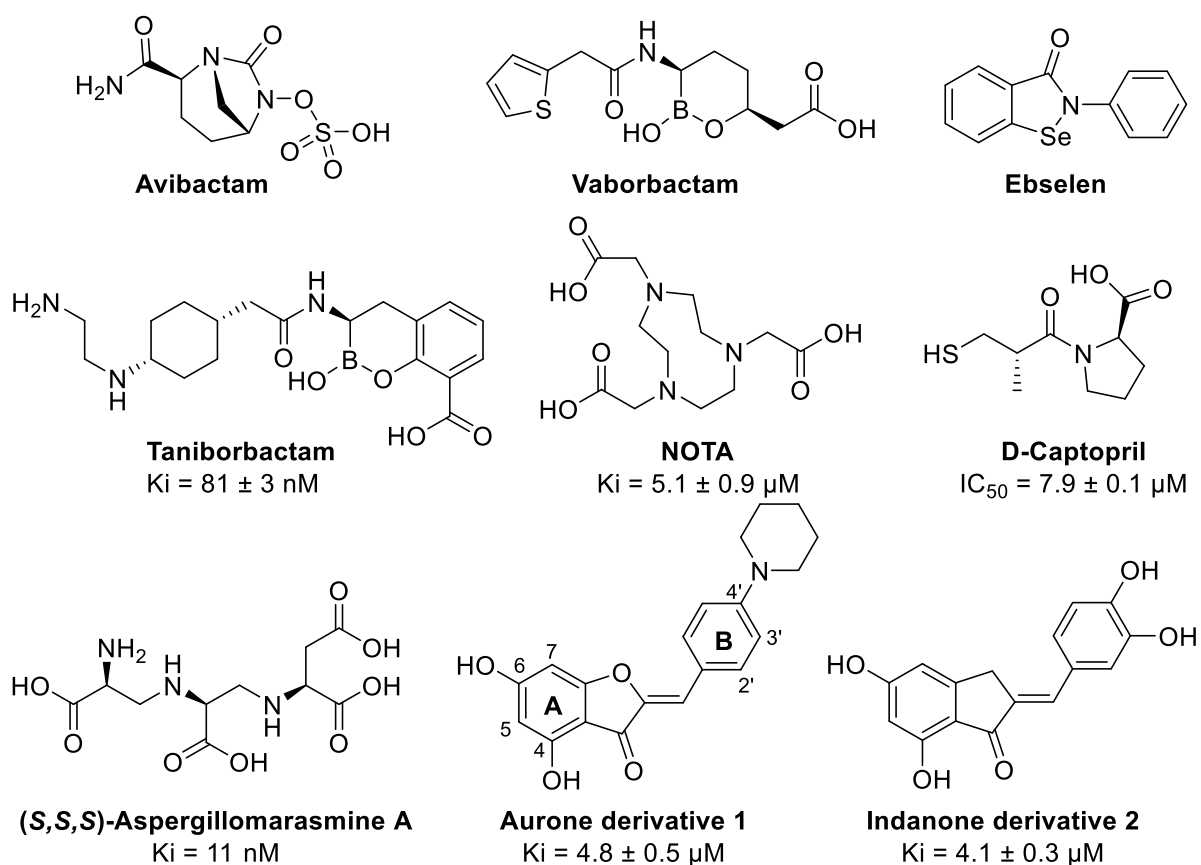


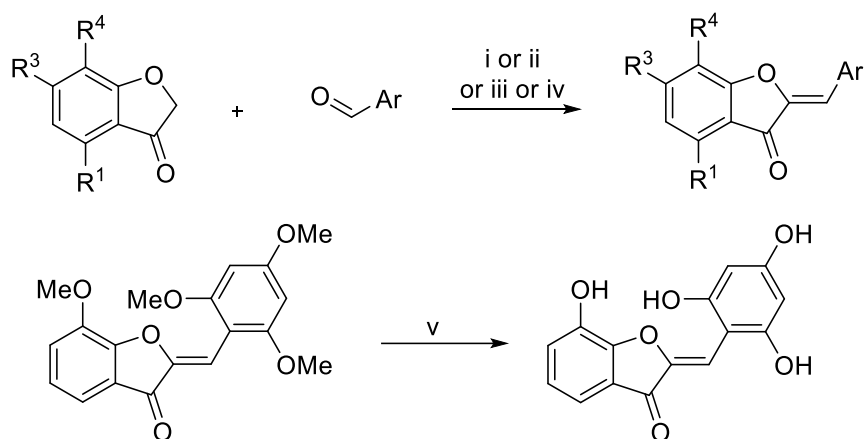
Figure 1. Structures of serine β -lactamases inhibitors (avibactam and vaborbactam) and of known NDM-1 inhibitors (A and B rings are specified on the aurone derivatives).

Indanones and aurones are structurally similar compounds: aurones are a subclass of the naturally occurring flavonoids while indanones are considered as the rigid cousins of chalcones, with an α,β -unsaturated ketone moiety [22]. In particular, aurones are minor natural products mostly occurring in some advanced plant species, and their therapeutic potential has only been investigated recently. Nevertheless, the aurone scaffold became more attractive as their low toxicity and broad spectrum of biological activities (e.g., anti-inflammatory, anticancer, antiviral, antibacterial, antispasmodic activities, potent antioxidative and antineurodegenerative effects [23–26]) progressively emerged.

Herein, to deepen our preliminary aurone hit identification (compound **1**), we report the synthesis and the structure-activity relationship (SAR) study of benzofuran-3(2*H*)-one derivatives, whose MBL inhibitory activity and spectrum were investigated using enzymatic (NDM-1, VIM-2, IMP-1) and microbiological assays.

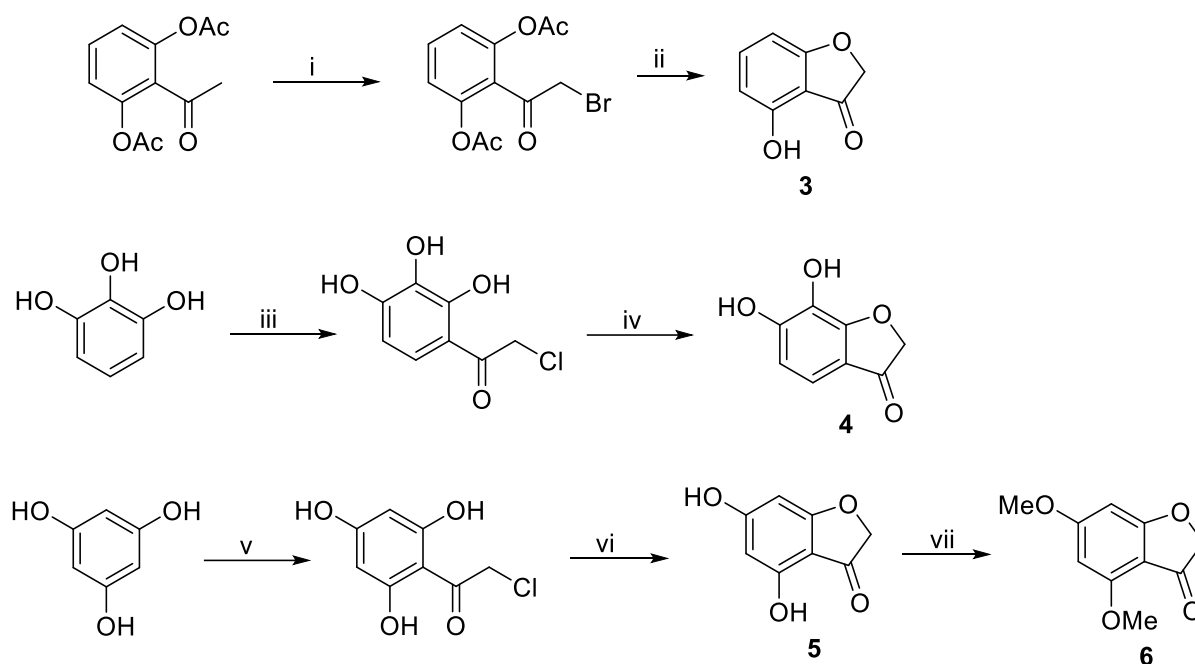
2. Chemistry

The aurone derivatives were synthesized using previously reported methods: they were prepared starting from substituted benzofuran-3(2*H*)-ones through an aldol condensation of various aryl aldehydes. The acidic, basic or neutral conditions of this reaction were chosen depending on the substituents present in both moieties (Scheme 1). When methoxy- or polymethoxy analogues were synthesized, an additional deprotection step to access to the hydroxy counterparts was necessary: boron tribromide in dichloromethane was used.



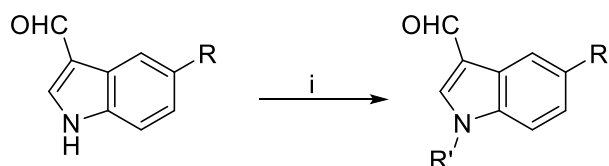
Scheme 1. General pathways for the synthesis of aurone derivatives. Reagents and conditions: (i) KOH/H₂O, MeOH or EtOH, 25–80 °C, 5 min to 2–7 h; (ii) ethylenediamine diacetate, MeCN, rt, ultrasound, 5–10 min; (iii) SOCl₂, MeOH, rt, 24–72 h; (iv) Al₂O₃, CH₂Cl₂, rt, overnight; (v) BBr₃, CH₂Cl₂, 0 °C, 24–96 h.

This convenient synthetic pathway is notably suitable for the simultaneous SAR exploration of the A and B rings of aurones but it requires the prior preparation of the properly substituted aryl aldehydes and benzofuran-3(2*H*)-ones that are not commercially available (Scheme 2). Compound **3** was obtained starting from the corresponding diacetoxyacetophenone after an α -bromination followed by a deprotection and cyclization sequence [27]. Compound **4** was synthesized via a Friedel-Crafts acylation starting from pyrogallol followed by a cyclization in basic conditions [28]. Compound **5** was synthesized starting from phloroglucinol, through a Houben-Hoesch reaction using chloroacetonitrile and zinc chloride in HCl / Et₂O, followed by simultaneous hydrolysis and cyclization in refluxed H₂O [29]. The methoxy analogue **6** was obtained using Me₂SO₄ in basic conditions.



Scheme 2. Synthesis of benzofuran-3(2*H*)-one cores **3–6** Reagents and conditions: (i) trimethylphenylammonium tribromide, THF, rt, 6 h; (ii) KOH/H₂O, MeOH, 65 °C, 3 h, 37% (for 2 steps); (iii) ClCH₂CO₂H, BF₃·Et₂O, 65 °C, 12 h, 73%; (iv) NaOAc, EtOH, reflux, 6 h, 91%; (v) ClCH₂CN, HCl, ZnCl₂, Et₂O, 0 °C, 3 h; (vi) HCl, H₂O, 100 °C, 1 h, 84% (for 2 steps); (vii) Me₂SO₄, K₂CO₃, 1,2-dimethoxyethane, reflux, 5 h, 97%.

Most of aryl aldehydes used in the aldol condensation were commercially available except the *N*-substituted indolecarboxaldehydes obtained by alkylation of the corresponding unsubstituted analogue with alkyl halides in the presence of sodium hydride (Scheme 3). When chloroalkane were used, KI was added to promote the nucleophilic substitution.



Scheme 3. Synthesis of indolecarboxaldehyde derivatives. Reagents and conditions: (i) R'X (X = Br, Cl), KI if X = Cl, NaH 60% in mineral oil, DMF, rt, 18–72 h.

3. Results and discussion

Using a spectrophotometric enzyme assay with purified MBL enzymes (see section 4.2. for details), the inhibitory activity of aurone derivatives were first assessed using a single fixed concentration of inhibitor (50 μM) in order to rapidly identify potentially interesting molecules (Table 1). Besides NDM-1, two other clinically relevant subclass B1 MBLs (VIM-2 and IMP-1) were included in the assay to determine the selectivity of these compounds. Indeed, if our derivatives were initially designed to target NDM-1 (because of their starting origin through the process of fragment identification and selection – FBDD strategy), broad-spectrum MBL inhibitors remain a desirable objective for efficiently hampering antibiotic resistance.

Tested derivatives included a total of 60 aurones – excluding the initial hit compound **1** – bearing modifications in the A, B or both rings, together with a series of B-heterocyclic indole analogues, allowing a better understanding of the structural requirements of MBL inhibition.

Starting from compound **1**, several 4'-substituted benzylidene 4,6-dihydroxybenzofuran-3(2*H*)-ones were tested. The exchange of 1-piperidinyl by cyclohexyl (**8**) led to a dramatic loss of activity, highlighting the major role of the *N*-heteroatom. Overall, all 4'-substituted analogues yielded a weaker activity than **1** at 50 μ M, but some compounds with various substituents maintained ~50% inhibition (**7**, **10** and **13**, with 4'-ethyl, 4'-1-imidazolyl and 4'-butoxy respectively). The introduction of hydroxy or methoxy substituents at positions 2' and 3' gave additional insights: if the presence of a methoxy group at position 3' appeared detrimental (**20** and **21** vs. **12**), compounds **15**, **16** and **19** indicated that the presence of a substituent at position 2' could provide a marginal to slightly beneficial impact on the recorded activity (**15** vs. **13**, **19** vs. **12**). In all cases, no activity was noticed on VIM-2 and only low or very low activities were found on IMP-1, except for compound **19** with relatively similar moderate activity on NDM-1 and IMP-1.

Modifications at the A-ring were then proposed. The 4,6-dimethoxy counterpart of compounds **19** and **21**, *i.e.* **22** and **23**, led to a completely abolished activity against NDM-1, while 2',4'-difluoro and 4'-2-thienyl derivatives **24** and **25** showed a residual effect. These observations could highlight the importance of the polyhydroxy substitution pattern at the A-ring, as confirmed by the results obtained from an alternative 6,7-dihydroxy series. Indeed, if compounds **26** and **28** were only found moderately active (especially when comparing **26** with **19**), the 2'-hydroxy-4'-methoxy analogue **27** reached a higher inhibition rate than the initial parent compound **1** (84.5% at 50 μ M). Interestingly, all the aurone derivatives with no or only one hydroxy substituent at the A-ring, regardless of its position, were found almost inactive (compounds **32–51**), thereby corroborating the importance of the polyhydroxy substitution pattern at the A-ring for an efficient interaction with NDM-1.

Replacing the B-ring by a heterocyclic indole-based counterpart followed a similar trend, as among the fifteen evaluated indolaurones (**52–66**), two of them (**65** and **66**) only presented one A-ring hydroxy group and revealed to be as well inactive. The activity level provided by the 4,6-dihydroxy analogues varied from very weak to significant inhibition (>68%) for the more active derivatives of this series (compounds **57–58** and **60–61**), whereas they demonstrated no activity against VIM-2 and low or intermediate inhibition against IMP-1. In particular, it is noteworthy that the presence of a bulky *N*-substituent was well tolerated at the indole core. That was especially the case with compound **57** which included a cyclohexyl group in this position and still exhibited a high inhibition level (more than 70%). Compounds **59–63**, with a substituted benzyl moiety on the indole nitrogen, displayed a variable activity that seemed to depend mainly on the position of the benzyl substituent. Higher activities were obtained when a substituent was present in *meta* position of the benzyl group (compounds **59–61**), and especially when the substituent was polar (**60–61** vs. **59**).

Table 1. Evaluation of the inhibitory activity of compounds **1** and **7–66** on NDM-1, VIM-2 and IMP-1 (the percentage of inhibition at 50 μ M was measured using enzyme assays, see Experimental section for details).

Cd	Structures					% inhibition ^a		
						NDM-1	VIM-2	IMP-1
1		R ^{2'}	R ^{3'}	R ^{4'}	R ^{5'}			
7		H	H	1-piperidinyl	H	74 \pm 5	17 \pm 6	20 \pm 5
8		H	H	Et	H	55 \pm 7	\leq 10	24.9 \pm 0.9
9		H	H	cyclohexyl	H	16 \pm 3	\leq 10	\leq 10
10		H	H	Cl	H	11 \pm 1	\leq 10	14 \pm 5
11		H	H	1-imidazolyl	H	51 \pm 6	\leq 10	23 \pm 5
12		H	H	OH	H	\leq 10	\leq 10	12.4 \pm 0.2
13		H	H	OMe	H	38 \pm 3	\leq 10	20 \pm 2
14		H	H	OBu	H	41 \pm 4	\leq 10	25 \pm 2
15		OH	H	OH	H	\leq 10	\leq 10	14 \pm 2
16		OH	H	OBu	H	46 \pm 6	n.d. ^a	n.d.
17		OH	H	N(Et) ₂	H	55 \pm 1	\leq 10	27 \pm 4
18		OH	H	H	H	\leq 10	\leq 10	14 \pm 4
19		OH	H	H	Me	\leq 10	\leq 10	12 \pm 3
20		OMe	H	OMe	H	52 \pm 5	\leq 10	43.6 \pm 0.6
21		H	OMe	OMe	H	23 \pm 6	\leq 10	21 \pm 6
21		OMe	OMe	OMe	H	14 \pm 4	\leq 10	20 \pm 5
22			R ^{2'}	R ^{3'}	R ^{4'}			
23			OMe	H	OMe	\leq 10	\leq 10	\leq 10
24			OMe	OMe	OMe	\leq 10	\leq 10	17 \pm 2
25			F	H	F	35 \pm 7	\leq 10	32 \pm 1
25	H	H	2-thienyl	39 \pm 5	\leq 10	24 \pm 6		
26		R ^{2'}	R ^{4'}					
27		OMe	OMe	30 \pm 3	10.3 \pm 0.1	28 \pm 4		
27		OH	OMe	84.5 \pm 0.8	\leq 10	49 \pm 2		
28		OH	OH	20 \pm 3	\leq 10	24 \pm 2		
29		H	CF ₃	\leq 10	\leq 10	17 \pm 2		
30	H	nBu	\leq 10	\leq 10	\leq 10			
31					50 \pm 6	\leq 10	19 \pm 6	
32		R ^{2'}	R ^{4'}	R ^{6'}				
32		H	OMe	H	20 \pm 4	\leq 10	\leq 10	
33		H	COOH	H	24 \pm 9	\leq 10	\leq 10	
34		OH	OH	OH	\leq 10	\leq 10	\leq 10	
35		OH	OH	H	\leq 10	\leq 10	\leq 10	
36		H	F	H	\leq 10	\leq 10	\leq 10	
37		H	Cl	H	\leq 10	\leq 10	\leq 10	

38		R ^{2'}	R ^{3'}	R ^{4'}	R ^{6'}			
39		H	OMe	OH	H	≤10	14 ± 5	13 ± 6
40		OMe	H	OMe	H	17 ± 3	≤10	17.9 ± 0.2
41		OH	H	OH	H	≤10	≤10	≤10
42		OMe	H	OH	H	≤10	≤10	13 ± 4
43		OH	H	OH	OH	≤10	≤10	≤10
44		OH	H	H	H	≤10	≤10	≤10
45						≤10	13 ± 6	15 ± 5
46		R ^{3'}	R ^{4'}					
47		OH	OH		12 ± 3	≤10	≤10	≤10
		H	4-Me-piperazinyl		≤10	≤10	≤10	12 ± 4
48		R ^{2'}	R ^{3'}	R ^{4'}				
49		OH	H	OH	≤10	≤10	≤10	
50		OMe	H	OH	≤10	≤10	≤10	
51		H	OMe	OH	≤10	≤10	≤10	
		OMe	OMe	OMe	≤10	≤10	≤10	
52		R ^{1'}		R				
53		Me		H	46 ± 6	≤10	28 ± 3	
54		CH ₂ CH=CH ₂		H	≤10	≤10	16 ± 2	
55		(S)-CH ₂ CH(CH ₃)CH ₂ CH ₃		H	49 ± 5	≤10	46 ± 3	
56		CH ₂ CH ₂ CH(CH ₃) ₂		H	18 ± 4	≤10	47.1 ± 0.8	
57		CH ₂ CH ₂ C(CH ₃) ₃		H	11.2 ± 0.2	≤10	28 ± 7	
58		CH ₂ cyclohexyl		H	72 ± 2	≤10	44 ± 2	
59		(CH ₂) ₃ Ph		H	68.7 ± 0.7	≤10	41 ± 2	
60		3-MeBn		H	54 ± 2	11.0 ± 0.8	43 ± 2	
61		3-HOBn		H	78 ± 3	≤10	31 ± 4	
62		3-BrBn		H	69 ± 2	≤10	43 ± 2	
63		4-BrBn		H	44 ± 5	≤10	22 ± 5	
64		2-BrBn		H	≤10	≤10	23 ± 2	
		Bu		OH	57 ± 4	≤10	30 ± 3	
65		R ⁴		R ⁶				
66		OH		H		≤10	≤10	21.4 ± 0.3
		H		OH		18 ± 3	≤10	39 ± 5
JMV-7061^b						97.0 ± 0.8	96.0 ± 0.9	40 ± 4
Taniborbactam^b						≥ 98	≥ 98	41 ± 2

^an.d.: Not determined

^bInhibition data for JMV-7061, a triazole-thione MBL inhibitor [30] and taniborbactam [31] are included for comparison and were tested at a final concentration of 100 and 50 μM , respectively. An additional inhibition control was 5 mM EDTA (observed inhibition for all tested enzymes, $\geq 95\%$).

Subsequently, the inhibition constants (K_i) were evaluated for the compounds displaying a percentage of inhibition higher than 65% at 50 μM (Table 2). Among these, aurone **27** and indolaurone derivative **57**, appeared to be the most promising compounds, with measured K_i on NDM-1 as low as 1.7 ± 0.2 and 2.5 ± 0.2 μM , respectively. The inhibition data allowing the determination of the K_i values (dependence of v_0/v_i as a function of inhibitor concentration) are in perfect agreement with a competitive model of inhibition (Figure S2). These five new compounds were also investigated for their ability to potentiate meropenem (a carbapenem antibiotic) in *in vitro* antimicrobial susceptibility assays on recent NDM-1- and NDM-4-producing extensively-drug resistant *Klebsiella pneumoniae* and *E. coli* clinical isolates. Unfortunately, their synergistic activity was rather modest, except for compound **57**, which showed an 8-fold decrease of meropenem MIC. The activity of this compound was also lower when tested on NDM-1- and NDM-4-producing *E. coli* isolates, highlighting the importance of the bacterial host, as well as the nature of the produced NDM-type variant. The overall modest potentiation of these compounds likely depends on either their modest potency (none of the K_i values are below the micromolar range) or their slow diffusion through the outer membrane, limiting their accumulation in the bacterial periplasm where their target is located. However, such data remain encouraging as they provide the experimental evidence that this scaffold could lead to compounds showing, besides their inhibitory activity in enzyme assays, the ability to reach and engage its target in the bacterial cell.

Table 2. Inhibition constants (K_i) and *in vitro* antibacterial synergistic activity with meropenem (MEM) of six representative most active compounds.

Cpd	NDM-1 K_i (μM)	MEM MIC ($\mu\text{g}/\text{mL}$) ^a		
		<i>K. pneumoniae</i> SI-518 ($bla_{\text{NDM-1}^+}$)	<i>E. coli</i> SI-004M ($bla_{\text{NDM-1}^+}$)	<i>E. coli</i> SI-G001 ($bla_{\text{NDM-4}^+}$)
None		128	64	128
1	4.8 ± 0.5	64	64	128
27	1.7 ± 0.2	32	32	128
57	2.5 ± 0.2	16	64	64
58	17 ± 3	32	32	64
60	16 ± 3	64	64	128
61	5.5 ± 0.6	32	32	64

^a *In vitro* susceptibility assays, the inhibitor was tested at a fixed concentration of 32 $\mu\text{g}/\text{mL}$ against three epidemiologically unrelated NDM-type MBL-producing strains. Compound JMV-7061, a triazole-thione MBL inhibitor [30], was used as the positive control of meropenem potentiation in these assays (MIC values when tested in the presence of 32 $\mu\text{g}/\text{mL}$ JMV-7061, ≤ 0.5 $\mu\text{g}/\text{mL}$).

Finally, a docking study was employed as the initial step in molecular modelling to explore the interactions between NDM-1 and the two most active compounds, **27** and **57**. We used this method, acknowledging its limitations in describing the binding mode when metal ions are present in the docking region. However, in conjunction with our biological results, it can help to identify interactions

with NDM-specific residues and large ligands, such as compounds **27** and **57**. We chose the crystallographic structure of NDM-1 with hydrolysed ampicillin as the co-crystallized ligand and a high resolution of 1 Å (PDB ID: 5ZGE). Different procedures were employed and are detailed in the computational section, particularly with or without the hydroxide ion from the crystallographic structure in the active site of NDM-1. Consistent results were obtained with the hydroxide ion in the active site (Figure 2). For these dockings with an excellent agreement obtained during the re-docking of the co-crystallized ligand (see Figure S1, in Supporting Information), the most populated clusters were the lowest energy one, containing a high number of conformers. Conversely, results obtained without the hydroxide anion showed greater variability and were inconclusive.

The analysis of the docked positions obtained for **27** and **57** highlighted several well-defined interactions, which provide a structural basis for the observed biochemical and biological results (Figure 2). Indeed, for compound **27**, three hydrogen-bond donors and/or acceptors were identified: one between the hydroxy group in position 5 and Glu152, one between the methoxy group and Asn220 and one between the oxygen of the carbonyl function and Asp124 – itself in bridged interaction with one Zn through the hydroxide ion present in the active site. The B-ring hydroxy group also interacts with the second Zn ion of the active site. Finally, a π -stacking interaction between the residue His122 and the aromatic A-ring of the aurone **27** was also observed. Regarding compound **57**, four hydrogen bond donors and/or acceptors were identified: these involved the four oxygens/hydroxy groups of the benzofuran core of compound **57** that interact with residues Gln123, Glu152, Asn220 and Asp223. π -Stacking interactions were also noticed between the ligand **57** and residues Trp93 and His122. In this case, no interaction was highlighted with the Zn ions but the complementary shape of the molecule and the active site is interesting to note, together with the relative space available to accommodate the cyclohexyl substituent. Furthermore, the binding of these compounds involves functionally important and conserved residues in NDM-type enzymes (e. g. Gln123, Glu152) and in other subclass B1 MBLs (e. g. His122, Asn220). The involvement of some NDM-specific residues in interacting with these potent inhibitors could explain, at least in part, their preferential inhibition of NDM-1 and the lack of activity on VIM-2.

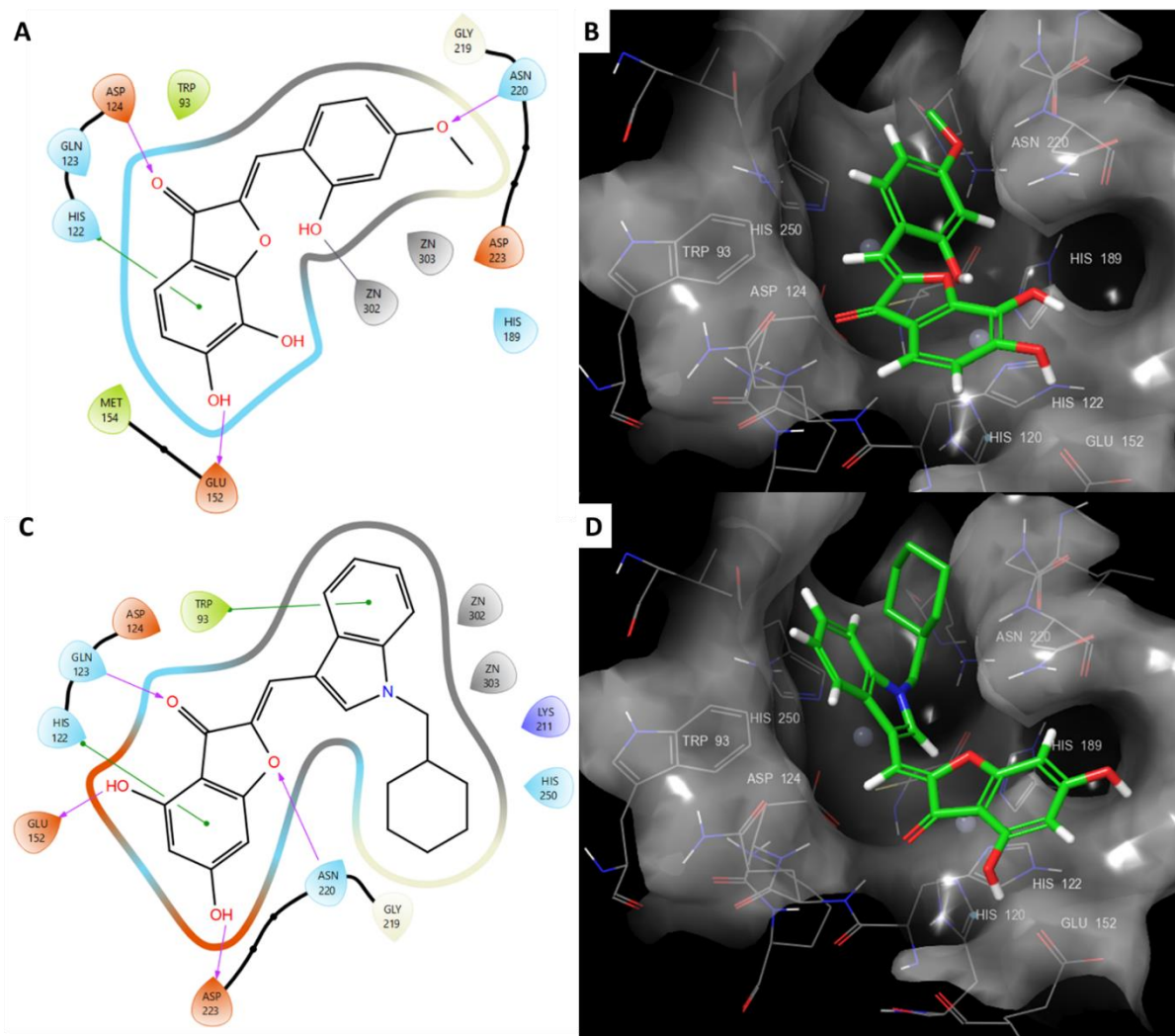


Figure 2. 2D map of interaction and 3D visualization of compounds **27** (A, B) and **57** (C, D) in the active site of NDM-1 (PDB 5ZGE); A,C: hydrogen bonds are indicated by a magenta arrow and pi-stacking interactions by a green line.

3. Conclusion

Following the discovery of a hit with a benzofuranone core, we evaluated the biochemical activity of 60 aurone derivatives to establish a structure-activity relationship study on NDM-1 and two other clinically relevant MBLs, namely IMP-1 and VIM-2. The five new compounds that have displayed the highest percentage of inhibition on NDM-1 were further studied. Compounds **27** and **57** were the best inhibitors of NDM-1, exhibiting inhibition constants in the micromolar range. *In vitro* antimicrobial susceptibility assays also demonstrated their ability to potentiate, although moderately, the antibacterial activity of meropenem on NDM-producing clinical isolates. Further modification of the compounds should indeed address the likely lack of diffusion through the bacterial outer membrane. Finally, molecular modelling allowed a better understanding of the interactions of these two compounds with important residues featured in the active site of NDM-1. The present biochemical and biological results, together with the analysis of their binding mode in NDM-1, will certainly support the synthesis of additional inhibitors, hopefully allowing the identification of better inhibitors, in terms of potency, spectrum of activity and synergistic activity in whole-cell assays.

In light of this, the pharmacomodulation of aurones and analogues will be pursued, building upon the acquired biochemical findings. The augmentation of experimental data will facilitate refining the molecular modelling protocol, enhancing the characterization of interactions between our ligands and NDM-1.

4. Experimental section

4.1. Chemistry

Unless stated otherwise, commercially available reagents and solvents were used without further purification. Reaction progress was monitored by Thin Layer Chromatography (TLC) on aluminium coated silica gel MN 60 F254 plates from Macherey-Nagel. The synthesized products were mostly purified by column chromatography on silica gel (MN Kieselgel 60 silica gel mesh size 63-200 μm). ^1H and ^{13}C Nuclear Magnetic Resonance (NMR) spectra were recorded in deuterated solvents at room temperature on a Bruker Avance 400 or Avance II 500 instruments. Chemical shifts (δ) are reported in parts per million (ppm) relative to TMS as internal standard or relative to the solvent [^1H : $\delta(\text{CDCl}_3) = 7.26$ ppm, $\delta(\text{DMSO-}d_6) = 2.50$ ppm, $\delta(\text{CD}_3\text{OD}) = 3.31$ ppm; ^{13}C : $\delta(\text{CDCl}_3) = 77.2$ ppm, $\delta(\text{DMSO-}d_6) = 39.5$ ppm, $\delta(\text{CD}_3\text{OD}) = 49.0$ ppm]. Multiplicity is reported as follows: bs, broad singlet; s, singlet; d, doublet; t, triplet and m, multiplet. Coupling constants J are given in Hertz. Electrospray Ionization (ESI) mass spectra and accurate mass measurements (HRMS) were acquired by NanoBio chemistry platform (ICMG FR2607). HPLC analyses were recorded on an Agilent 1260 Infinity II using a diode array detector and a C18 reversed-phase column (Zorbax Eclipse plus C18, Agilent, 3-5 μm particle size, 100 mm \times 2.1 mm) at 30 $^\circ\text{C}$, with a mobile phase A composed of water and formic acid 0.1 % and a phase mobile B composed of MeOH and formic acid 0.1 % with a three steps elution (90:10 A:B over 2 min, then a gradient 90:10 to 0:100 over 12 min and finally 0:100 over 2 min), detection at 254 nm. Purity of all the tested compounds was $\geq 95\%$. The synthesis and characterization of compounds **1–9**, **11–14**, **18–19**, **21–22**, **28**, **33**, **35–37**, **39–48**, **52–53**, **57–61** and **64** have already been reported elsewhere [27,29,32–41].

4.1.1. General procedure A. To a solution of substituted benzofuran-3(2*H*)-one (1 equiv.) in ethanol (3 mL/mmol) were added an aqueous solution of KOH (50%, 5 mL/mmol) and an arylaldehyde (1.0 to 3.5 equiv.). The solution was refluxed until TLC showed complete disappearance of the starting material (2 to 5 h). After cooling, ethanol was removed under reduced pressure, then the residue was diluted into distilled water (50 mL/mmol) and an aqueous solution of hydrochloric acid (10%) was added to adjust the pH to 2–3. The mixture was then extracted with CH_2Cl_2 or EtOAc. The combined organic layers were washed with water and brine, dried over MgSO_4 , filtered off and concentrated under reduced pressure to afford the corresponding arylidene derivative. The crude product was finally purified by flash chromatography or by recrystallization in MeOH.

4.1.2. General procedure B. To a solution of 4,6-dimethoxybenzofuran-3(2*H*)-one **6** (1 equiv.) in CH_2Cl_2 (15 mL/mmol) were added a benzaldehyde derivative (1.2 equiv.) and Al_2O_3 (36 equiv.). The suspension was stirred at rt under nitrogen overnight, then filtered and concentrated. The product was recrystallized in MeOH and filtered off to afford the corresponding benzylidene derivative.

4.1.3. *General procedure C.* To a solution of substituted benzofuran-3(2*H*)-one (1 equiv.) in MeOH (15 mL/mmol) were added an arylaldehyde derivative (1.5 equiv.) and then dropwise an aqueous solution of KOH 50% (1.5 mL/mmol). After stirring for 3 to 7 h at reflux, the reaction mixture was cooled for 30 min in an ice bath and the precipitate was filtered off and washed with cold water and MeOH; if necessary, the product was purified by a recrystallisation in MeOH.

4.1.4. *General procedure D.* To a solution of a benzofuran-3(2*H*)-one in MeOH (10 mL/mmol) were added an aqueous solution of KOH (50%, 5 mL/mmol) and a benzaldehyde (1 equiv.), and the mixture was stirred at 25–40 °C until solid appearance. The precipitate was filtered, washed with cold MeOH and hot H₂O, and dried to afford the corresponding crude aurone.

4.1.5. *General procedure E.* To a solution of a polymethoxyaurone derivative in dry CH₂Cl₂ (10 mL/mmol) was added a solution of BBr₃ in CH₂Cl₂ (1 M, 10–20 equiv.) at 0 °C, and the mixture was stirred at room temperature for 24–96 h. Iced water was then added and the suspension was stirred at room temperature for 1 h. The mixture was extracted three times with AcOEt. The combined organic layers were dried over MgSO₄, filtered, and the filtrate was concentrated under reduced pressure to afford the corresponding crude polyhydroxyaurone.

4.1.6. *General procedure F.* To a solution of a benzofuran-3(2*H*)-one in MeOH (3 mL/mmol) were added an aqueous solution of KOH (50%, 5 mL/mmol) and a benzaldehyde (1–2 equiv.), and the mixture was refluxed for 2–5 h. After cooling, MeOH was removed under reduced pressure, then the residue was diluted in H₂O (50 mL/mmol). An aqueous solution of HCl (10%) was added until pH 1–2, and the mixture was extracted three times with AcOEt. The combined organic layers were washed with H₂O and brine, dried over MgSO₄, filtered, and the filtrate was concentrated under reduced pressure to afford the corresponding crude aurone.

4.1.7. *General procedure G.* To a solution of a benzofuran-3(2*H*)-one derivative in MeCN (15 mL/mmol) were added ethylenediamine diacetate (1.2 equiv.) and a benzaldehyde (1 equiv.), and the mixture was stirred at room temperature under ultrasound until solid appearance (5–10 min). The precipitate was filtered, washed with MeCN and hot H₂O, and dried to afford the corresponding crude aurone.

4.1.8. *General procedure H.* To a solution of a benzofuran-3(2*H*)-one derivative in MeOH (15 mL/mmol) were added SOCl₂ (1.5 equiv.) dropwise and a benzaldehyde (1 equiv.), and the mixture was stirred at room temperature for 24–72 h. The mixture was concentrated under reduced pressure, then the residue was washed with cold MeOH and hot H₂O, and dried to afford the corresponding crude aurone.

4.1.9. *General procedure I.* To a suspension of NaH 60% in oil (2.25 equiv.) in dry DMF (0.8 mL/mmol) was added, at 0 °C and under nitrogen atmosphere, a solution of indolecarboxaldehyde (1 equiv.) in dry DMF (2.5 mL/mmol). After stirring for 30 min at rt, alkyl halide (1.0–3.0 equiv.) was slowly added. If alkyl chloride was used, KI was added (1.0 equiv.). After stirring overnight, the reaction was quenched by addition of water and the product was extracted with diethyl ether. The organic layer was dried over MgSO₄, filtered off and concentrated under vacuum. The crude product was purified by column chromatography on silica gel.

4.1.10. *(Z)*-2-(4-(1*H*-imidazol-1-yl)benzylidene)-4,6-dihydroxybenzofuran-3(2*H*)-one (**10**). The crude product was prepared according to the general procedure A starting from **5** (100 mg, 0.60 mmol) and 4-(1*H*-imidazol-1-yl)benzaldehyde (250 mg, 1.45 mmol). After purification by column

chromatography, the pure product (169 mg, 0.53 mmol, 88%) was obtained as a yellow powder. ¹H NMR (400 MHz, DMSO-*d*₆) δ ppm 11.00 (s, 1H), 10.93 (s, 1H), 8.37 (s, 1H), 8.03 (d, *J* = 8.7 Hz, 2H), 7.88-7.75 (m, 3H), 7.15 (s, 1H), 6.68 (s, 1H), 6.25 (d, *J* = 1.7 Hz, 1H), 6.09 (d, *J* = 1.7 Hz, 1H); ¹³C NMR (101 MHz, DMSO-*d*₆) δ ppm 178.9 (C), 167.8 (C), 167.5 (C), 158.5 (C), 147.9 (C), 136.8 (C), 132.1 (CH), 132.1 (2xCH), 130.9 (C), 130.1 (CH), 120.3 (2xCH), 117.8 (CH), 107.1 (CH), 102.5 (C), 97.8 (CH), 90.7 (CH); LRMS (ESI⁺) *m/z* (%) 321 [M+H]⁺ (100); HRMS (ESI⁺) *m/z* calc. for C₁₈H₁₃N₂O₄ 321.0869, found 321.0866.

4.1.11. (*Z*)-2-(4-Butoxy-2-hydroxybenzylidene)-4,6-dihydroxybenzofuran-3(2H)-one (**15**). The crude product was prepared according to the general procedure A starting from **5** (100 mg, 0.60 mmol) and 4-butoxy-2-hydroxybenzaldehyde [42] (200 mg, 1.03 mmol). After column chromatography, the pure product (115 mg, 0.34 mmol, 56%) was obtained as a yellow powder. ¹H NMR (400 MHz, DMSO-*d*₆) δ ppm 10.77 (bs, 2H), 10.29 (s, 1H), 7.96 (d, *J* = 8.8 Hz, 1H), 6.88 (s, 1H), 6.53 (dd, *J* = 8.8, 2.4 Hz, 1H), 6.47 (d, *J* = 2.4 Hz, 1H), 6.18 (d, *J* = 1.7 Hz, 1H), 6.06 (d, *J* = 1.7 Hz, 1H), 3.95 (t, *J* = 6.5 Hz, 2H), 1.74-1.64 (m, 2H), 1.48-1.37 (m, 2H), 0.93 (t, *J* = 7.4 Hz, 3H); ¹³C NMR (101 MHz, DMSO-*d*₆) δ ppm 179.0 (C), 167.4 (C), 166.8 (C), 160.9 (C), 158.4 (C), 158.1 (C), 145.8 (C), 131.8 (CH), 112.1 (C), 106.8 (C), 103.0 (CH), 102.9 (C), 101.2 (CH), 97.6 (CH), 90.4 (CH), 67.2 (CH₂), 30.6 (CH₂), 18.7 (CH₂), 13.7 (CH₃); LRMS (ESI⁺) *m/z* (%) 343 [M+H]⁺ (100); HRMS (ESI⁻) *m/z* calc. for C₁₉H₁₇O₆ 341.1031, found 341.1020.

4.1.12. (*Z*)-2-(4-(Diethylamino)-2-hydroxybenzylidene)-4,6-dihydroxybenzofuran-3(2H)-one (**16**). The crude product was prepared according to the general procedure A starting from **5** (100 mg, 0.60 mmol) and 4-diethylamino-2-hydroxybenzaldehyde (250 mg, 1.29 mmol). After purification by column chromatography, the pure product (74 mg, 0.22 mmol, 36%) was obtained as a brown powder. ¹H NMR (400 MHz, DMSO-*d*₆) δ ppm 10.61 (bs, 2H), 9.86 (s, 1H), 7.89 (d, *J* = 9.0 Hz, 1H), 6.90 (s, 1H), 6.31 (dd, *J* = 9.0, 2.1 Hz, 1H), 6.22-6.13 (m, 2H), 6.03 (d, *J* = 1.6 Hz, 1H), 3.41-3.26 (m, 4H), 1.11 (t, *J* = 7.0 Hz, 6H); ¹³C NMR (101 MHz, DMSO-*d*₆) δ ppm 178.7 (C), 166.9 (C), 166.2 (C), 158.7 (C), 157.7 (C), 149.9 (C), 144.3 (C), 132.1 (CH), 106.9 (C), 104.8 (CH), 104.34 (CH) 103.4 (C), 97.3 (CH), 97.1 (CH), 90.2 (CH), 43.9 (CH₂), 12.6 (CH₃); LRMS (ESI⁺) *m/z* (%) 342 [M+H]⁺ (100); HRMS (ESI⁺) *m/z* calc. for C₁₉H₂₀NO₅ 342.1336, found 342.1333.

4.1.13. (*Z*)-2-(2-Hydroxy-5-methylbenzylidene)-4,6-dihydroxybenzofuran-3(2H)-one (**17**). The crude product was prepared according to the general procedure A starting from **5** (100 mg, 0.60 mmol) and 2-hydroxy-5-methylbenzaldehyde (250 mg, 1.84 mmol). After purification by column chromatography, the pure product (94 mg, 0.33 mmol, 55%) was obtained as a yellow powder. ¹H NMR (400 MHz, DMSO-*d*₆) δ ppm 10.97-10.79 (m, 2H), 9.97 (s, 1H), 7.82 (s, 1H), 7.10-6.98 (m, 1H), 6.90 (s, 1H), 6.82 (d, *J* = 8.2 Hz, 1H), 6.22 (s, 1H), 6.08 (s, 1H), 2.26 (s, 3H); ¹³C NMR (100 MHz, DMSO-*d*₆) δ ppm 179.1 (C), 167.7 (C), 167.2 (C), 158.3 (C), 154.6 (C), 147.0 (C), 131.5 (CH), 130.6 (CH), 127.9 (C), 118.9 (C), 115.5 (CH), 102.7 (C), 102.6 (CH), 97.7 (CH), 90.6 (CH), 20.4 (CH₃); LRMS (ESI⁺) *m/z* (%) 285 [M+H]⁺ (95), 307 [M+Na]⁺ (100); HRMS (ESI⁻) *m/z* calc. for C₁₆H₁₁O₅ 283.0612, found 283.0605.

4.1.14. (*Z*)-2-(3,4-Dimethoxybenzylidene)-4,6-dihydroxybenzofuran-3(2H)-one (**20**). The crude product was prepared according to the general procedure A starting from **5** (100 mg, 0.60 mmol) and 3,4-dimethoxybenzaldehyde (200 mg, 1.20 mmol). After purification by column chromatography, the pure product (138 mg, 0.44 mmol, 73%) was obtained as a yellow powder. ¹H NMR (400 MHz, DMSO-*d*₆) δ ppm 10.86 (bs, 2H), 7.55-7.46 (m, 2H), 7.10-7.02 (m, 1H), 6.58 (s, 1H), 6.22 (d, *J* = 1.7 Hz, 1H), 6.07 (d, *J* = 1.7 Hz, 1H), 3.90-3.75 (m, 6H); ¹³C NMR (101 MHz, DMSO-*d*₆) δ ppm 179.0 (C), 167.6 (C), 167.1 (C), 158.2 (C), 149.9 (C), 148.7 (C), 146.5 (C), 125.1 (C), 124.4 (CH), 113.9 (CH), 111.9 (CH), 108.9 (CH), 102.7

(C), 97.7 (CH), 90.6 (CH), 55.6 (CH₃), 55.5 (CH₃); LRMS (ESI⁺) *m/z* (%) 315 [M+H]⁺ (100); HRMS (ESI⁺) *m/z* calc. for C₁₇H₁₅O₆ 315.0863, found 315.0864.

4.1.15. (*Z*)-2-(2,3,4-Trimethoxybenzylidene)-4,6-dimethoxybenzofuran-3(2*H*)-one (**23**). The crude product was prepared according to the general procedure B starting from **6** (100 mg, 0.52 mmol) and 2,3,4-trimethoxybenzaldehyde (121 mg, 0.62 mmol). The pure product (74 mg, 0.20 mmol, 38%) was obtained as an orange powder. ¹H NMR (400 MHz, DMSO-*d*₆) δ ppm 7.90 (d, *J* = 9.0 Hz, 1H), 6.96 (d, *J* = 9.0 Hz, 1H), 6.82 (s, 1H), 6.67 (t, *J* = 1.8 Hz, 1H), 6.34 (d, *J* = 1.8 Hz, 1H), 3.89 (m, 12H), 3.78 (s, 3H); ¹³C NMR (101 MHz, DMSO-*d*₆) δ ppm 178.8 (C), 168.7 (C), 168.0 (C), 158.9 (C), 155.0 (C), 152.8 (C), 146.8 (C), 141.7 (C), 126.0 (CH), 118.3 (C), 108.5 (CH), 104.1 (C), 103.1 (CH), 94.4 (CH), 89.9 (CH), 61.6 (CH₃), 60.5 (CH₃), 56.5 (CH₃), 56.1 (CH₃), 56.1 (CH₃); LRMS (ESI⁺) *m/z* (%) 373 [M+H]⁺ (100); HRMS (ESI⁺) *m/z* calc. for C₂₀H₂₁O₇ 373.1282, found 373.1278.

4.1.16. (*Z*)-2-[(2,4-Difluorobenzylidene)-4,6-dimethoxybenzofuran-3(2*H*)-one (**24**). The crude product was prepared according to the general procedure B starting from **6** (100 mg, 0.52 mmol) and 2,4-difluorobenzaldehyde (70 μL, 0.62 mmol). After purification by recrystallization in MeOH, the pure product (66 mg, 0.21 mmol, 41%) was obtained as a yellow solid. R_f 0.67 (cyclohexane/EtOAc 6:4); ¹H NMR (CDCl₃, 400 MHz) δ ppm 8.19-8.25 (m, 1H), 6.93-6.97 (m, 2H), 6.83-6.88 (m, 1H), 6.35 (s, 1H), 6.12 (s, 1H), 3.94 (s, 3H), 3.90 (s, 3H); ¹³C NMR (CDCl₃, 100 MHz) δ ppm 180.2 (C), 169.2 (C), 169.0 (C), 163.3 (dd, *J* = 253, 12 Hz, C), 161.8 (dd, *J* = 253, 12 Hz, C), 159.6 (C), 148.5 (C), 132.7 (dd, *J* = 10, 3 Hz, CH), 117.4 (dd, *J* = 22, 4 Hz, C), 112.0 (dd, *J* = 22, 4 Hz, CH), 105.1 (C), 104.1 (t, *J* = 25 Hz, CH), 100.9 (dd, *J* = 7, 2 Hz, CH), 94.3 (CH), 89.4 (CH), 56.4 (CH₃), 56.3 (CH₃); LRMS (ESI⁺) *m/z* (%) 319 [M+H]⁺ (100), 341 [M+Na]⁺ (43), 337 [M+K]⁺ (57); HRMS (ESI⁻) *m/z* calc. for C₁₇H₁₃O₄F₂ 319.0776, found 319.0770.

4.1.17. (*Z*)-2-[(4-(2-Thienyl)benzylidene)-4,6-dimethoxybenzofuran-3(2*H*)-one (**25**). The crude product was prepared according to the general procedure C starting from compound **6** (100 mg, 0.52 mmol) and 4-(2-thienyl)benzaldehyde (145 mg, 0.77 mmol). After purification by recrystallization in MeOH, the pure product (139 mg, 0.38 mmol, 74%) was obtained as an orange powder. R_f 0.16 (cyclohexane/EtOAc 6:4); ¹H NMR (CDCl₃, 400 MHz) δ ppm 7.89 (d, *J* = 8.4 Hz, 2H), 7.69 (d, *J* = 8.4 Hz, 2H), 7.40 (d, *J* = 3.6 Hz, 1H), 7.34 (d, *J* = 5.0 Hz, 1H), 7.12 (dd, *J* = 5.0, 3.6 Hz, 1H), 6.79 (s, 1H), 6.42 (d, *J* = 1.7 Hz, 1H), 6.16 (d, *J* = 1.7 Hz, 1H), 3.98 (s, 3H), 3.94 (s, 3H); ¹³C NMR (CDCl₃, 100 MHz) δ ppm 180.8 (C), 169.2 (2xC), 159.7 (C), 148.1 (C), 143.9 (C), 135.3 (C), 131.9 (C), 131.9 (2xCH), 128.5 (CH), 126.2 (2xCH), 125.8 (CH), 124.0 (CH), 110.5 (CH), 105.5 (C), 94.3 (CH), 89.5 (CH), 56.5 (CH₃), 56.4 (CH₃); HRMS (ESI⁺) *m/z* calc. for C₂₁H₁₇O₄S 365.0842, found 365.0843.

4.1.18. (*Z*)-2-(2,4-Dimethoxybenzylidene)-6,7-dihydroxybenzofuran-3(2*H*)-one (**26**). The crude product was prepared according to the general procedure A starting from **4** (166 mg, 1.00 mmol) and 2,4-dimethoxybenzaldehyde (200 mg, 1.20 mmol). After purification by column chromatography, the pure product (214 mg, 0.68 mmol, 68%) was obtained as a yellow powder. ¹H NMR (400 MHz, DMSO-*d*₆) δ ppm 10.61 (bs, 1H), 9.57 (bs, 1H), 8.32 (d, *J* = 8.7 Hz, 1H), 7.12 (d, *J* = 8.3 Hz, 1H), 7.02 (s, 1H), 6.75-6.69 (m, 2H), 6.67 (d, *J* = 2.4 Hz, 1H), 3.91 (s, 3H), 3.86 (s, 3H); ¹³C NMR (101 MHz, DMSO-*d*₆) δ ppm 182.0 (C), 162.3 (C), 159.8 (C), 154.9 (C), 154.3 (C), 146.3 (C), 132.7 (CH), 130.1 (C), 115.3 (CH), 114.4 (C), 113.2 (C), 112.7 (CH), 106.6 (CH), 104.1 (CH), 98.1 (CH), 55.9 (CH₃), 55.5 (CH₃); LRMS (ESI⁺) *m/z* (%) 315 [M+H]⁺ (100); HRMS (ESI⁻) *m/z* calc. for C₁₇H₁₃O₆ 313.0718, found 313.0711.

4.1.19. (*Z*)-2-(2-Hydroxy-4-methoxybenzylidene)-6,7-dihydroxybenzofuran-3(2*H*)-one (**27**). The crude product was prepared according to the general procedure A starting from **4** (100 mg, 0.60 mmol) and

2-hydroxy-4-methoxybenzaldehyde (120 mg, 0.79 mmol). After purification by column chromatography, the pure product (117 mg, 0.39 mmol, 65%) was obtained as a red powder. ¹H NMR (400 MHz, DMSO-*d*₆) δ ppm 8.25 (d, *J* = 8.8 Hz, 1H), 7.11 (d, *J* = 8.3 Hz, 1H), 7.06 (s, 1H), 6.72 (d, *J* = 8.3 Hz, 1H), 6.58 (dd, *J* = 8.8, 2.5 Hz, 1H), 6.50 (d, *J* = 2.5 Hz, 1H), 3.77 (s, 3H); ¹³C NMR (101 MHz, DMSO-*d*₆) δ ppm 181.9 (C), 16.02 (C), 158.9 (C), 154.8 (C), 154.1 (C), 145.8 (C), 132.7 (CH), 130.1 (C), 115.2 (CH), 114.6 (C), 112.6 (CH), 112.1 (C), 106.6 (CH), 105.1 (CH), 100.6 (CH), 55.2 (CH₃); LRMS (ESI⁺) *m/z* (%) 301 [M+H]⁺ (100); HRMS (ESI⁻) *m/z* calc. for C₁₆H₁₁O₆ 299.0561, found 299.0553.

4.1.20. 2-(4-Trifluoromethylbenzylidene)-6,7-dihydroxybenzofuran-3(2H)-one (**29**). The crude product was prepared according to the general procedure A starting from **4** (0.2 g, 1.2 mmol) and 4-trifluoromethylbenzaldehyde (269 mg, 1.8 mmol). After purification by column chromatography, the pure product (152 mg, 0.47 mmol, 39%) was obtained as an orange powder. ¹H NMR (400 MHz, CD₃OD) δ ppm 8.19 (d, *J* = 8.4 Hz, 2H), 7.75 (d, *J* = 8.0 Hz, 2H), 7.22 (d, *J* = 8.0 Hz, 1H), 6.81 (s, 1H), 6.74 (d, *J* = 8.4 Hz, 1H); ¹³C NMR (100 MHz, CD₃OD) δ ppm 185.1 (C), 157.3 (C), 157.0 (C), 150.8 (C), 137.8 (C), 132.8 (4xCH), 131.6 (CH), 128.8 (C), 126.8 (q, *J* = 32 Hz, CF₃), 126.7 (CH), 117.5 (C), 115.7 (CH), 114.1 (CH); HRMS (ESI⁺) *m/z* calc. for C₁₆H₁₀FO₄ 323.0525, found 323.0524.

4.1.21. (Z)-2-(4-Butylbenzylidene)-6,7-dihydroxybenzofuran-3(2H)-one (**30**). The crude product was prepared according to the general procedure A starting from **4** (100 mg, 0.60 mmol) and 4-butylbenzaldehyde (200 mg, 1.23 mmol). After purification by column chromatography, the pure product (125 mg, 0.40 mmol, 67%) was obtained as a red powder. ¹H NMR (400 MHz, DMSO-*d*₆) δ ppm 7.95 (d, *J* = 8.2 Hz, 2H), 7.32 (d, *J* = 8.2 Hz, 2H), 7.14 (d, *J* = 8.3 Hz, 1H), 6.79-6.71 (m, 2H), 2.63 (t, *J* = 7.6 Hz, 2H), 1.63-1.53 (m, 2H), 1.37-1.26 (m, 2H), 0.90 (t, *J* = 7.3 Hz, 3H); ¹³C NMR (101 MHz, DMSO-*d*₆) δ ppm 182.2 (C), 155.2 (C), 154.7 (C), 147.2 (C), 144.5 (C), 131.3 (2xCH), 130.1 (C), 129.7 (C), 128.9 (2xCH), 115.5 (CH), 114.2 (C), 112.8 (CH), 110.5 (CH), 34.8 (CH₂), 32.9 (CH₂), 21.7 (CH₂), 13. (CH₃); LRMS (ESI⁺) *m/z* (%) 311 [M+H]⁺ (100); HRMS (ESI⁻) *m/z* calc. for C₁₉H₁₇O₄ 309.1132, found 309.1125.

4.1.22. 2-(2'-Naphthylmethylene)-6,7-dihydroxybenzofuran-3(2H)-one (**31**). The crude product was prepared according to the general procedure A starting from **4** (0.2 g, 1.2 mmol) and 2-naphthaldehyde (282 mg, 1.8 mmol). After purification by column chromatography on silica gel (EtOAc/cyclohexane), the pure product (169 mg, 0.55 mmol, 46%) was obtained as an orange powder. ¹H NMR (400 MHz, DMSO-*d*₆) δ ppm 8.52 (s, 1H), 8.22 (dd, *J* = 1.6, *J* = 4.0, 1H), 8.02 (s, 1H), 8.00 (s, 1H), 7.98-7.94 (m, 2H), 7.59-7.57 (m, 3H), 7.15 (d, *J* = 8.0 Hz, 1H), 6.88 (s, 1H), 6.69 (d, *J* = 8.4 Hz, 1H); ¹³C NMR (100 MHz, DMSO-*d*₆) δ ppm 182.2 (C), 155.2 (C), 154.9 (C), 147.8 (C), 133.0 (CH), 132.9 (C), 131.6 (C), 130.0 (C), 129.8 (CH), 128.4 (CH), 128.3 (CH), 127.6 (2xCH), 127.4 (CH), 126.7 (C), 115.6 (CH), 114.0 (C), 112.9 (CH), 110.3 (CH); HRMS (ESI⁺) *m/z* calc. for C₁₉H₁₃O₄ 305.0808, found 305.0803.

4.1.23. (Z)-7-Hydroxy-2-(2,4,6-trihydroxybenzylidene)benzofuran-3(2H)-one (**34**) – 2 steps

4.1.23.1. (Z)-7-Methoxy-2-(2,4,6-trimethoxybenzylidene)benzofuran-3(2H)-one (**34a**). The crude product was prepared according to the general procedure D starting from 7-methoxybenzofuran-3(2H)-one (100 mg, 0.609 mmol) and 2,4,6-trimethoxybenzaldehyde (120 mg, 0.609 mmol). The product (29 mg, 0.085 mmol, 14%) was obtained as a yellow powder. ¹H NMR (400 MHz, DMSO-*d*₆) δ ppm 7.38 (dd, *J* = 7.3, 1.0 Hz, 1H), 7.29 (dd, *J* = 7.3, 1.0 Hz, 1H), 7.18 (t, *J* = 7.3 Hz, 1H), 6.90 (s, 1H), 6.34 (s, 2H), 3.93 (s, 3H), 3.86 (s, 3H), 3.85 (s, 6H). ¹³C NMR (100 MHz, DMSO-*d*₆) δ ppm 183.3, 163.4, 159.9, 145.6, 145.6, 123.8, 122.6, 119.5, 115.1, 106.2, 102.1, 91.3, 56.5, 56.0, 55.6. HRMS (ESI⁺) *m/z* calc. for C₁₉H₁₉O₆ (M+H)⁺ 343.1176, found 343.1173.

4.1.23.2. *(Z)*-7-Hydroxy-2-(2,4,6-trihydroxybenzylidene)benzofuran-3(2H)-one (**34**). The crude product was prepared according to the general procedure E starting from **34a** (29 mg, 0.085 mmol). After purification by column chromatography on silica gel (eluent CH₂Cl₂/MeOH), the product (20 mg, 0.070 mmol, 82%) was obtained as a yellow powder. ¹H NMR (400 MHz, CD₃OD) δ ppm 7.42 (s, 1H), 7.23 (d, *J* = 7.6 Hz, 1H), 7.13 (d, *J* = 7.6 Hz, 1H), 7.06 (t, *J* = 7.6 Hz, 1H), 5.98 (s, 2H); ¹³C NMR (100 MHz, CD₃OD) δ ppm 185.4, 163.8, 160.3, 154.4, 144.8, 144.7, 125.2, 124.7, 123.8, 115.2, 110.2, 101.7, 96.5. HRMS (ESI⁻) *m/z* calc. for C₁₅H₉O₆ (M-H)⁻ 285.0405, found 285.0405.

4.1.24. *(Z)*-6-Hydroxy-2-(4-hydroxy-3-methoxybenzylidene)benzofuran-3(2H)-one (**38**). The crude product was prepared according to the general procedure F starting from 6-hydroxybenzofuran-3(2H)-one (200 mg, 1.33 mmol) and 4-hydroxy-3-methoxybenzaldehyde (240 mg, 1.33 mmol). The product (336 mg, 1.18 mmol, 89%) was obtained as an orange powder. ¹H NMR (400 MHz, DMSO-*d*₆) δ ppm 11.12 (s, 1H), 9.76 (s, 1H), 7.60 (d, *J* = 8.3 Hz, 1H), 7.53 (d, *J* = 1.9 Hz, 1H), 7.48 (dd, *J* = 8.3, 1.9 Hz, 1H), 6.90 (d, *J* = 8.3 Hz, 1H), 6.80 (d, *J* = 1.9 Hz, 1H), 6.74 (s, 1H), 6.71 (dd, *J* = 8.3, 1.9 Hz, 1H), 3.84 (s, 3H). ¹³C NMR (100 MHz, DMSO-*d*₆) δ ppm 181.1, 167.4, 166.0, 148.8, 147.7, 145.7, 125.6, 125.3, 123.3, 116.0, 115.0, 113.1, 112.8, 111.6, 98.5, 55.6. HRMS (ESI⁺) *m/z* calc. for C₁₆H₁₃O₅ (M+H)⁺ 285.0758, found 285.0753.

4.1.25. *(Z)*-2-(4-Hydroxy-2-methoxybenzylidene)benzofuran-3(2H)-one (**49**). The crude product was prepared according to the general procedure G starting from benzofuran-3(2H)-one (100 mg, 0.746 mmol) and 4-hydroxy-2-methoxybenzaldehyde (113 mg, 0.746 mmol). The product (137 mg, 0.511 mmol, 69%) was obtained as a yellow powder. ¹H NMR (400 MHz, DMSO-*d*₆) δ ppm 8.10 (d, *J* = 8.6 Hz, 1H), 7.76 (m, 2H), 7.53 (d, *J* = 8.4 Hz, 1H), 7.29 (t, *J* = 7.5 Hz, 1H), 7.18 (s, 1H), 6.55 (dd, *J* = 8.6, 2.2 Hz, 1H), 6.50 (d, *J* = 2.2 Hz, 1H), 3.86 (s, 3H). ¹³C NMR (100 MHz, DMSO-*d*₆) δ ppm 182.8, 164.7, 162.5, 160.6, 144.5, 136.8, 132.9, 124.0, 123.6, 121.4, 113.1, 111.1, 109.0, 107.0, 99.2, 55.7. HRMS (ESI⁺) *m/z* calc. for C₁₆H₁₃O₄ 269.0808, found 269.0813.

4.1.26. *(Z)*-2-(4-Hydroxy-3-methoxybenzylidene)benzofuran-3(2H)-one (**50**). The crude product was prepared according to the general procedure H starting from benzofuran-3(2H)-one (200 mg, 1.49 mmol) and 4-hydroxy-3-methoxybenzaldehyde (269 mg, 1.49 mmol). The product (304 mg, 1.13 mmol, 76%) was obtained as an orange powder. ¹H NMR (400 MHz, DMSO-*d*₆) δ ppm 9.88 (s, 1H), 7.78 (m, 2H), 7.60 (d, *J* = 1.8 Hz, 1H), 7.55 (m, 2H), 7.30 (t, *J* = 7.4 Hz, 1H), 6.92 (m, 2H), 3.86 (s, 3H). ¹³C NMR (100 MHz, DMSO-*d*₆) δ ppm 183.1, 165.0, 149.4, 147.8, 144.8, 137.1, 126.1, 124.1, 123.7, 123.3, 121.3, 116.1, 115.4, 113.8, 113.2, 55.7. HRMS (ESI⁺) *m/z* calc. for C₁₆H₁₃O₄ 269.0808, found 269.0806.

4.1.27. *(Z)*-2-[(3,4,5-Trimethoxy)phenylmethylene]benzofuran-3(2H)-one (**51**). The crude product was prepared according to the general procedure A starting from benzofuran-3(2H)-one (100 mg, 0.75 mmol) and 3,4,5-trimethoxybenzaldehyde (176 mg, 0.89 mmol). The pure product (198 mg, 0.63 mmol, 85%) was obtained as a yellow powder. R_f 0.28 (cyclohexane/EtOAc 8:2); ¹H NMR (400 MHz, CDCl₃) δ ppm 7.81 (dd, *J* = 7.5, 1.4 Hz, 1H), 7.65 (ddd, *J* = 8.3, 7.5, 1.4 Hz, 1H), 7.30 (d, *J* = 8.3 Hz, 1H), 7.23 (dd, *J* = 7.5, 7.5 Hz, 1H), 7.18 (s, 2H), 6.82 (s, 1H), 3.94 (s, 6H), 3.92 (s, 3H); ¹³C NMR (100 MHz, CDCl₃) δ ppm 184.7 (C), 166.0 (C), 153.4 (2xC), 146.5 (C), 140.1 (C), 136.9 (CH), 127.8 (C), 124.8 (CH), 123.7 (CH), 121.8 (C), 113.5 (CH), 113.0 (CH), 109.0 (2xCH), 61.2 (CH₃), 56.3 (2xCH₃); LRMS (ESI⁺) *m/z* (%) 338 (100) [M+H]⁺; HRMS (ESI⁺) *m/z* calc. for C₁₉H₁₆NO₅ 338.1028, found 338.1030.

4.1.28. *(S,Z)*-4,6-Dihydroxy-2-((1-(2-methylbutyl)-1H-indol-3-yl)methylene)benzofuran-3(2H)-one (**54**)
– 2 steps

4.1.28.1. *(S)*-1-(2-Methylbutyl)-1H-indole-3-carbaldehyde (**54a**). The crude product was prepared according to the general procedure I starting from 1H-indole-3-carbaldehyde (650 mg, 4.48 mmol) and (*S*)-1-bromo-2-methylbutane (0.90 g, 5.96 mmol). The product (644 mg, 2.99 mmol, 68%) was obtained as a yellow oil. ¹H NMR (400 MHz, CDCl₃) δ ppm 10.00 (s, 1H), 8.34-8.28 (m, 1H), 7.68 (s, 1H), 7.40-7.27 (m, 3H), 4.10 (dd, *J* = 14.1, 6.7 Hz, 1H), 3.90 (dd, *J* = 14.1, 8.1 Hz, 1H), 2.10-1.96 (m, 1H), 1.49-1.37 (m, 1H), 1.30-1.17 (m, 1H), 0.96 (t, *J* = 7.4 Hz, 3H), 0.91 (d, *J* = 6.7 Hz, 3H); ¹³C NMR (100 MHz, CDCl₃) δ ppm 184.7 (CH), 139.0 (C), 137.7 (C), 125.6 (C), 124.0 (CH), 123.0 (CH), 122.3 (CH), 118.1 (CH), 110.4 (CH), 53.6 (CH₂), 35.6 (CH), 27.2 (CH₂), 17.3 (CH₃), 11.3 (CH₃); LRMS (ESI⁺) *m/z* (%) 216 [M+H]⁺ (100); HRMS (ESI⁺) *m/z* calc. for C₁₄H₁₈ON 216.1383, found 216.1380.

4.1.28.2. *(S,Z)*-4,6-Dihydroxy-2-((1-(2-methylbutyl)-1H-indol-3-yl)methylene)benzofuran-3(2H)-one (**54**). The crude product was prepared according to the general procedure A starting from **5** (100 mg, 0.60 mmol) and (*S*)-1-(2-methylbutyl)-1H-indole-3-carbaldehyde **54a** (350 mg, 1.63 mmol). After purification by column chromatography, the pure product (129 mg, 0.35 mmol, 59%) was obtained as a yellow powder. ¹H NMR (400 MHz, DMSO-*d*₆) δ ppm 10.81-10.59 (m, 2H), 8.09 (s, 1H), 7.97 (d, *J* = 7.7 Hz, 1H), 7.57 (d, *J* = 8.1 Hz, 1H), 7.30-7.22 (m, 1H), 7.22-7.13 (m, 1H), 6.96 (s, 1H), 6.25 (s, 1H), 6.07 (s, 1H), 4.21 (dd, *J* = 13.9, 6.9 Hz, 1H), 4.09 (dd, *J* = 13.9, 7.9 Hz, 1H), 1.98 (dd, *J* = 11.1, 6.1 Hz, 1H), 1.42-1.28 (m, 1H), 1.25-1.10 (m, 1H), 0.89 (t, *J* = 7.3 Hz, 3H), 0.82 (d, *J* = 6.5 Hz, 3H); ¹³C NMR (101 MHz, DMSO-*d*₆) δ ppm 178.3 (C), 166.9 (C), 166.5 (C), 157.9 (C), 145.3 (C), 136.4 (C), 133.3 (CH), 127. (C), 122.5 (CH), 120.6 (CH), 119.1 (CH), 110.8 (CH), 107.3 (C), 103.6 (C), 102.1 (CH), 97.5 (CH), 90.4 (CH), 51.9 (CH₂), 35.2 (CH), 26.3 (CH₂), 16.6 (CH₃), 11.0 (CH₃); LRMS (ESI⁺) *m/z* (%) 364 [M+H]⁺; HRMS (ESI⁺) *m/z* calc. for C₂₂H₂₀NO₄ 362.1398, found 362.1391.

4.1.29. *(Z)*-4,6-Dihydroxy-2-((1-isopentyl-1H-indol-3-yl)methylene)benzofuran-3(2H)-one (**55**). The crude product was prepared according to the general procedure A starting from **5** (100 mg, 0.60 mmol) and 1-isopentyl-1H-indole-3-carbaldehyde (350 mg, 1.63 mmol). After purification by column chromatography, the pure product (135 mg, 0.37 mmol, 62%) was obtained as an orange powder. ¹H NMR (400 MHz, DMSO-*d*₆) δ ppm 10.83-10.57 (m, 2H), 8.13 (s, 1H), 7.97 (d, *J* = 7.2 Hz, 1H), 7.55 (d, *J* = 7.5 Hz, 1H), 7.32-7.12 (m, 2H), 6.95 (s, 1H), 6.25 (s, 1H), 6.07 (s, 1H), 4.45-4.20 (m, 2H), 1.82-1.64 (m, 2H), 1.64-1.45 (m, 1H), 1.05-0.87 (d, *J* = 5.6 Hz, 6H); ¹³C NMR (101 MHz, DMSO-*d*₆) δ ppm 178.3 (C), 166.9 (C), 166.5 (C), 157.9 (C), 145.3 (C), 135.8 (C), 132.8 (CH), 127.2 (C), 122.5 (CH), 120.6 (CH), 119.1 (CH), 110.5 (CH), 107.4 (C), 103.7 (C), 102.1 (CH), 97.5 (CH), 90.4 (CH), 44.5 (CH₂), 38.5 (CH₂), 25.3 (CH), 22.3 (CH₃); LRMS (ESI⁺) *m/z* (%) 364 [M+H]⁺; HRMS (ESI⁺) *m/z* calc. for C₂₂H₂₀NO₄ 364.1543, found 364.1541.

4.1.30. *(Z)*-2-((1-(3,3-Dimethylbutyl)-1H-indol-3-yl)methylene)-4,6-dihydroxybenzofuran-3(2H)-one (**56**) – 2 steps

4.1.30.1. 1-(3,3-Dimethylbutyl)-1H-indole-3-carbaldehyde (**56a**). The crude product was prepared according to the general procedure I starting from 1H-indole-3-carbaldehyde (650 mg, 4.48 mmol) and 1-chloro-3,3-dimethylbutane (1.0 g, 8.29 mmol). The product (750 mg, 3.27 mmol, 73%) was obtained as a light pink powder. ¹H NMR (400 MHz, CDCl₃) δ ppm 10.00 (s, 1H), 8.28-8.23 (m, 1H), 7.74 (s, 1H), 7.39-7.29 (m, 3H), 4.22-4.15 (m, 2H), 1.85-1.78 (m, 2H), 1.05 (s, 9H); ¹³C NMR (100 MHz, CDCl₃) δ ppm 184.6 (CH), 138.1 (C), 137.3 (C), 125.7 (C), 124.1 (CH), 123.1 (CH), 122.4 (CH), 118.4 (CH), 110.1 (CH), 44.1 (CH), 43.7 (CH), 30.2 (C), 29.4 (3xCH₃); LRMS (ESI⁺) *m/z* (%) 230 [M+H]⁺ (100); HRMS (ESI⁺) *m/z* calc. for C₁₉H₂₀ON (M+H)⁺ 230.1539, found 230.1538.

4.1.30.2. (*Z*)-2-((1-(3,3-Dimethylbutyl)-1*H*-indol-3-yl)methylene)-4,6-dihydroxybenzofuran-3(2*H*)-one (**56**). The crude product was prepared according to the general procedure A starting from **5** (100 mg, 0.60 mmol) and 1-(3,3-dimethylbutyl)-1*H*-indole-3-carbaldehyde **56a** (370 mg, 1.61 mmol). After purification by column chromatography, the pure product (147 mg, 0.39 mmol, 65%) was obtained as an orange powder. ¹H NMR (400 MHz, DMSO-*d*₆) δ ppm 10.71 (s, 1H), 10.66 (s, 1H), 8.15 (s, 1H), 7.97 (d, *J* = 7.8 Hz, 1H), 7.50 (d, *J* = 8.1 Hz, 1H), 7.27 (m, 1H), 7.19 (m, 1H), 6.95 (s, 1H), 6.26 (s, 1H), 6.07 (s, 1H), 4.41-4.21 (m, 2H), 1.80-1.62 (m, 2H), 1.01 (s, 9H); ¹³C NMR (101 MHz, DMSO-*d*₆) δ ppm 178.3 (C), 166.9 (C), 166.5 (C), 157.8 (C), 145.2 (C), 135.7 (C), 132.8 (CH), 127.3 (C), 122.5 (CH), 120.6 (CH), 119.1 (CH), 110.4 (CH), 107.4 (C), 103.6 (C), 102.1 (CH), 97.5 (CH), 90.4 (CH), 43.1 (CH₂), 42.9 (CH₂), 29.8 (C), 29.1 (CH₃); LRMS (ESI⁺) *m/z* (%) 378 [M+H]⁺ (100); HRMS (ESI⁻) *m/z* calc. for C₂₃H₂₂BrNO₄ 376.1554, found 376.1547.

4.1.31. (*Z*)-2-((1-(4-Bromobenzyl)-1*H*-indol-3-yl)methylene)-4,6-dihydroxybenzofuran-3(2*H*)-one (**62**). The crude product was prepared according to the general procedure A starting from **5** (100 mg, 0.60 mmol) and 1-(4-bromobenzyl)-1*H*-indole-3-carbaldehyde (400 mg, 1.27 mmol). After purification by column chromatography, the pure product (171 mg, 0.37 mmol, 62%) was obtained as an orange powder. ¹H NMR (400 MHz, DMSO-*d*₆) δ ppm 10.86-10.60 (m, 2H), 8.30 (s, 1H), 7.98 (d, *J* = 7.0 Hz, 1H), 7.57-7.45 (m, 3H), 7.25-7.14 (m, 4H), 6.97 (s, 1H), 6.22 (s, 1H), 6.06 (s, 1H), 5.57 (s, 2H); ¹³C NMR (101 MHz, DMSO-*d*₆) δ ppm 178.1 (C), 166.7 (C), 166.3 (C), 157.7 (C), 145.3 (C), 136.7 (C), 135.6 (C), 132.9 (CH), 131.3 (2xCH), 129.0 (2xCH), 127.2 (C), 122.5 (CH), 120.6 (CH), 120.4 (C), 118.9 (CH), 110.6 (CH), 107.7 (C), 103.3 (C), 101.5 (CH), 97.3 (CH), 90.1 (CH), 48.6 (CH₂); LRMS (ESI⁺) *m/z* (%) 462 [M+H]⁺ for ⁷⁹Br (100), 464 [M+H]⁺ for ⁸¹Br (98); HRMS (ESI⁻) *m/z* calc. for C₂₄H₁₅BrNO₄ 460.0190 (⁷⁹Br), found 460.0187.

4.1.32. (*Z*)-2-((1-(2-Bromobenzyl)-1*H*-indol-3-yl)methylene)-4,6-dihydroxybenzofuran-3(2*H*)-one (**63**). The crude product was prepared according to the general procedure A starting from **5** (100 mg, 0.60 mmol) and 1-(2-bromobenzyl)-1*H*-indole-3-carbaldehyde (400 mg, 1.27 mmol). After purification by column chromatography, the pure product (152 mg, 0.33 mmol, 55%) was obtained as a yellow powder. ¹H NMR (400 MHz, DMSO-*d*₆) δ ppm 10.79-10.67 (m, 2H), 8.24 (s, 1H), 8.02 (dd, *J* = 5.9, 2.9 Hz, 1H), 7.72 (dd, *J* = 7.4, 1.5 Hz, 1H), 7.44 (dd, *J* = 6.1, 2.7 Hz, 1H), 7.31-7.18 (m, 4H), 6.99 (s, 1H), 6.66 (dd, *J* = 7.2, 1.9 Hz, 1H), 6.17 (d, *J* = 1.2 Hz, 1H), 6.06 (d, *J* = 1.2 Hz, 1H), 5.63 (s, 2H); ¹³C NMR (101 MHz, DMSO-*d*₆) δ ppm 178.3 (C), 166.9 (C), 166.6 (C), 157.9 (C), 145.7 (C), 136.2 (C), 136.1 (C), 133.2 (CH), 132.8 (CH), 129.7 (CH), 128.3 (CH), 128.2 (CH), 127.3 (C), 122.9 (CH), 122.0 (C), 121.0 (CH), 119.2 (CH), 110.7 (CH), 108.2 (C), 103.6 (C), 101.7 (CH), 97.5 (CH), 90.3 (CH), 49.8 (CH₂); LRMS (ESI⁺) *m/z* (%) 462 [M+H]⁺ for ⁷⁹Br (100), 464 [M+H]⁺ for ⁸¹Br (98); HRMS (ESI⁻) *m/z* calc. for C₂₄H₁₅BrNO₄ 460.0190 (⁷⁹Br), found 460.0188.

4.1.33. (*Z*)-2-(*N*-Methyl-5-bromoindol-3-ylmethylene)-4-hydroxybenzofuran-3(2*H*)-one (**65**). The crude product was prepared according to the general procedure A (except that EtOH was replaced by MeOH 15 mL/mmol) starting from 4-hydroxybenzofuran-3(2*H*)-one **5** (50 mg, 0.33 mmol) and *N*-methyl-5-bromoindole-3-carboxaldehyde [43] (119 mg, 0.50 mmol). After purification by recrystallization in MeOH, the pure product (64 mg, 0.17 mmol, 52%) was obtained as an orange powder. R_f 0.24 (cyclohexane/EtOAc 6:4); ¹H NMR (400 MHz, CDCl₃) δ ppm 8.03 (d, *J* = 1.8 Hz, 1H), 7.97 (s, 1H), 7.96 (bs, 1H), 7.48 (dd, *J* = 8.2, 8.2 Hz, 1H), 7.41 (dd, *J* = 8.6, 1.8 Hz, 1H), 7.24 (d, *J* = 8.6 Hz, 1H), 7.18 (s, 1H), 6.80 (d, *J* = 8.2 Hz, 1H), 6.61 (d, *J* = 8.2 Hz, 1H), 3.91 (s, 3H); ¹³C NMR (101 MHz, CDCl₃) δ ppm 184.2 (C), 164.0 (C), 156.7 (C), 144.9 (C), 138.3 (CH), 135.9 (C), 135.5 (CH), 129.5 (C), 126.3 (CH), 122.2 (CH),

115.2 (C), 111.6 (CH), 110.8 (C), 109.5 (CH), 108.2 (C), 106.3 (CH), 103.5 (CH), 33.9 (CH₃); LRMS (ESI⁻) *m/z* (%) 369 [M-H⁺] (100); HRMS (ESI⁻) *m/z* calc. for C₁₈H₁₂BrNO₃ 370.0079, found 370.0100.

4.1.34. (*Z*)-2-(*N*-Methyl-5-bromoindol-3-ylmethylene)-6-hydroxybenzofuran-3(2*H*)-one (**66**). The crude product was prepared according to the general procedure A starting from commercially available 6-hydroxybenzofuran-3(2*H*)-one (158 mg, 1.05 mmol) and *N*-methyl-5-bromoindole-3-carboxaldehyde [43] (500 mg, 2.10 mmol). After purification by recrystallization in MeOH, the pure product (300 mg, 0.81 mmol, 77%) was obtained as a yellow powder. *R*_f 0.23 (cyclohexane/EtOAc 6:4); ¹H NMR (400 MHz, DMSO-*d*₆) δ ppm 8.30 (d, *J* = 1.8 Hz, 1H), 8.24 (s, 1H), 7.59 (d, *J* = 8.4 Hz, 1H), 7.54 (d, *J* = 8.7 Hz, 1H), 7.40 (dd, *J* = 8.7, 1.8 Hz, 1H), 7.19 (s, 1H), 6.78 (d, *J* = 1.9 Hz, 1H), 6.69 (dd, *J* = 8.4, 1.9 Hz, 1H), 3.93 (s, 3H); ¹³C NMR (101 MHz, DMSO-*d*₆) δ ppm 180.2 (C), 166.7 (C), 165.9 (C), 145.3 (C), 135.8 (C), 135.6 (CH), 128.9 (C), 125.5 (CH), 125.1 (CH), 121.8 (CH), 114.0 (C), 113.8 (C), 112.8 (CH), 112.7 (CH), 107.0 (C), 104.2 (CH), 98.4 (CH), 33.4 (CH₃); LRMS (ESI⁻) *m/z* (%) 370 [M-H⁺] (100); HRMS (ESI⁻) *m/z* calc. for C₁₈H₁₂BrNO₃ 370.0079, found 370.0100.

4.2. Enzyme inhibition assays

The NDM-1, VIM-2 and IMP-1 metallo-β-lactamases were produced and purified as previously described [21]. The inhibitory activity of synthesized compounds was evaluated using spectrophotometric assays and the reporter substrate method. The hydrolysis rate of 150 μM imipenem (used as the reporter substrates) was monitored by following the time-dependence variation of absorbance (300 nm) in both the absence and presence of compounds, in 50 mM HEPES buffer (pH 7.5) supplemented with 0.1 % Triton X-100 (this detergent was added to limit the potential identification of pan-assay interference compounds [PAINS]). Compounds were initially resuspended in DMSO (100 mM) and subsequently diluted in the reaction buffer. The percentage of inhibition on NDM-1 was computed using the following formula: 100 - [100 × (*v*_i / *v*₀)], where *v*₀ and *v*_i are the hydrolysis rates of the reporter substrate in the absence and presence of 50 μM compound, respectively. All measurements were performed at least in triplicate. Positive controls of inhibition were 5 mM EDTA, 100 μM JMV-7061 [30] and 50 μM taniborbactam (DBA Italia S.r.l., Segrate, Italy). NDM-1 inhibition constants (*K*_i values) were determined using a competitive inhibition model by measuring the initial reaction rate of hydrolysis of the reporter substrate (150 μM imipenem) in 50 mM HEPES buffer (pH, 7.5) by means of spectrophotometric assays, in the absence and presence of a variable concentration of inhibitor and by plotting the *v*₀ / *v*_i ratio vs compound concentration:

$$\frac{v_0}{v_i} = 1 + \frac{K_M}{(K_M + [S]) K_i} \cdot [I]$$

where [S] is the concentration of reporter substrate, [I] the concentration of the tested compound and *K*_M the Michaelis constant of the enzyme for the reporter substrate (NDM-1 *K*_M for imipenem hydrolysis, 80 μM). *K*_i values were computed as *K*_M / [(*K*_M + [S]) × slope]. All assays were performed in triplicate.

4.3. In vitro antimicrobial susceptibility testing

The potential synergistic activity of selected compounds was evaluated on *K. pneumoniae* and *E. coli* NDM-1- and NDM-4-producing clinical isolates (strains SI-518, SI-004M and SI-G001) [44] by measuring the minimum inhibitory concentrations (MICs) of meropenem in both the absence and presence of a fixed concentration (32 µg/mL) of an inhibitor (compound JMV-7061 [30] was used as the positive control in these experiments). MICs were determined in triplicate using Mueller-Hinton broth and a bacterial inoculum of 5×10^4 CFU/well, as recommended by the CLSI [45]. The stock solutions of the antibiotic (1.2 mg/mL in sterile milliQ water) and compounds (3.2 mg/mL in DMSO) were diluted in the growth medium. For assessing the activity of the combination, the inhibitor was added at 32 µg/mL to the wells immediately prior to the addition of the antibiotic diluted in growth medium containing 32 µg/mL inhibitor and the two-fold serial dilutions. Bacterial suspensions were added extemporaneously to each well, prior to incubation of the plates at 35 ± 2 °C for 24 h. Results were read following visual inspection of the plates.

4.4. Molecular modeling

The crystallographic structure of NDM-1 (PDB ID: 5ZGE) was recovered from RCSB Protein Data Bank (<https://www.rcsb.org/pdb>) as a dimeric form of NDM-1 containing hydrolyzed ampicillin ligand in its active site. The protein monomer was prepared by removing the B subunit of 5ZGE, the hydrolyzed ampicillin molecule and water molecules. This structure contains also a hydroxide anion, close to zinc atoms in the active site. Docking studies were performed with and without this hydroxide anion in the active site. The monomeric form of NDM-1 is a 241 amino acids long single chain polypeptide bearing Glu30 as N-terminal residue and Arg270 as C-terminal residue. Polar hydrogen atoms and Kollman charges were added to the protein using AutoDock Tools 1.5.6 [46]. For docking with the hydroxide anion in the active site, we used standard autodock parameters for zinc atoms with two sets of charges added manually. In the first set, we assign a charge of +2 to the Zn ion and -1 to the hydroxide anion. The second set corresponds to Mulliken charges attributed to the Zn, O and H atoms. These charges are obtained with DFT calculation at b3lyp/6-31G(d,p) level on a cluster model of the active site, taking into account the first coordination sphere of zinc atoms. Same binding modes were obtained with the two sets with a high number of conformers in the clusters. For docking without the hydroxide anion, two parameters were also used. We tested the force field adapted to Zinc atoms of AutDock4_{Zn} [47] with a charge of +2 to the Zn ion and 0 to the Zn pseudo atom added. We also used a standard autodock parameters for zinc atoms with a charge of +2.

For all calculations, the grid calculation was performed by AutoGrid4 and consisted of a 70 x 70 x 70 points grid for x, y and z dimensions with spacing of 0.200 Å centered on the coordinates Zn₁ (2.281, 45.278, 110.757 for the x, y and z-axes respectively). Grid maps were generated for aromatic carbons (A), aliphatic carbons (C), polar hydrogens (HD), hydrogen-bond acceptor oxygen (OA), aliphatic nitrogen (N), aromatic nitrogen (NA) and bromine (Br). Sulfur map (SA) was calculated for the hydrolyzed ampicillin ligand redocking. The ligands were built using GaussView16 [48] and their geometry was optimized using Gaussian16, with b3lyp as hybrid functional and 6-31G(d,p) as basis set. Non-polar hydrogen atoms were removed and Kollman charges were added to the ligands using AutoDock Tools 1.5.6.

Prepared ligands were docked into the generated grid maps using AutoDock 4.2.6 [46]. The docking was set to 50 runs and each were ranked by cluster with a RMSD tolerance of 2.0 Å.

Ligands-protein interactions were visualized using Maestro software [49].

Declaration of Competing Interest

The authors declare no known competing interests that could have influence the work reported here.

Acknowledgments

This work has been partially supported by Labex Arcane and CBH-EUR-GS (ANR-17-EURE-0003). The authors wish to acknowledge the ICMG Nanobio Platform (FR 2607), on which the NMR and MS experiments were performed.

Appendix A. Supplementary data

Supplementary data related to this article can be found at [doi](#)

References

- [1] C.L. Ventola, The antibiotic resistance crisis: part 1: causes and threats, *P T Peer-Rev. J. Formul. Manag.* 40 (2015) 277–283.
- [2] C.J. Murray, K.S. Ikuta, F. Sharara, L. Swetschinski, G. Robles Aguilar, A. Gray, C. Han, C. Bisignano, P. Rao, E. Wool, S.C. Johnson, A.J. Browne, M.G. Chipeta, F. Fell, S. Hackett, G. Haines-Woodhouse, B.H. Kashef Hamadani, E.A.P. Kumaran, B. McManigal, R. Agarwal, S. Akech, S. Albertson, J. Amuasi, J. Andrews, A. Aravkin, E. Ashley, F. Bailey, S. Baker, B. Basnyat, A. Bekker, R. Bender, A. Bethou, J. Bielicki, S. Boonkasidecha, J. Bukosia, C. Carvalheiro, C. Castañeda-Orjuela, V. Chansamouth, S. Chaurasia, S. Chiurchiù, F. Chowdhury, A.J. Cook, B. Cooper, T.R. Cressey, E. Criollo-Mora, M. Cunningham, S. Darboe, N.P.J. Day, M. De Luca, K. Dokova, A. Dramowski, S.J. Dunachie, T. Eckmanns, D. Eibach, A. Emami, N. Feasey, N. Fisher-Pearson, K. Forrest, D. Garrett, P. Gastmeier, A.Z. Giref, R.C. Greer, V. Gupta, S. Haller, A. Haselbeck, S.I. Hay, M. Holm, S. Hopkins, K.C. Iregbu, J. Jacobs, D. Jarovsky, F. Javanmardi, M. Khorana, N. Kissoon, E. Kobeissi, T. Kostyanev, F. Krapp, R. Krumkamp, A. Kumar, H.H. Kyu, C. Lim, D. Limmathurotsakul, M.J. Loftus, M. Lunn, J. Ma, N. Mturi, T. Munera-Huertas, P. Musicha, M.M. Mussi-Pinhata, T. Nakamura, R. Nanavati, S. Nangia, P. Newton, C. Ngoun, A. Novotney, D. Nwakanma, C.W. Obiero, A. Olivas-Martinez, P. Olliaro, E. Ooko, E. Ortiz-Brizuela, A.Y. Peleg, C. Perrone, N. Plakkal, A. Ponce-de-Leon, M. Raad, T. Ramdin, A. Riddell, T. Roberts, J.V. Robotham, A. Roca, K.E. Rudd, N. Russell, J. Schnall, J.A.G. Scott, M. Shivamallappa, J. Sifuentes-Osornio, N. Steenkeste, A.J. Stewardson, T. Stoeva, N. Tasak, A. Thaiprakong, G. Thwaites, C. Turner, P. Turner, H.R. van Doorn, S. Velaphi, A. Vongpradith, H. Vu, T. Walsh, S. Waner, T. Wangrangsimakul, T. Wozniak, P. Zheng, B. Sartorius, A.D. Lopez, A. Stergachis, C. Moore, C. Dolecek, M. Naghavi, Global burden of bacterial antimicrobial resistance in 2019: a systematic analysis, *The Lancet.* 399 (2022) 629–655. [https://doi.org/10.1016/S0140-6736\(21\)02724-0](https://doi.org/10.1016/S0140-6736(21)02724-0).
- [3] K. Garber, A β -lactamase inhibitor revival provides new hope for old antibiotics, *Nat. Rev. Drug Discov.* 14 (2015) 445–447. <https://doi.org/10.1038/nrd4666>.
- [4] A.S. Chaudhary, A review of global initiatives to fight antibiotic resistance and recent antibiotics' discovery, *Acta Pharm. Sin. B.* 6 (2016) 552–556. <https://doi.org/10.1016/j.apsb.2016.06.004>.

- [5] K.A. Toussaint, J.C. Gallagher, β -Lactam/ β -Lactamase Inhibitor Combinations: From Then to Now, *Ann. Pharmacother.* 49 (2015) 86–98. <https://doi.org/10.1177/1060028014556652>.
- [6] P.W. Groundwater, S. Xu, F. Lai, L. Váradi, J. Tan, J.D. Perry, D.E. Hibbs, New Delhi metallo- β -lactamase-1: structure, inhibitors and detection of producers, *Future Med. Chem.* 8 (2016) 993–1012. <https://doi.org/10.4155/fmc-2016-0015>.
- [7] R. Cain, J. Brem, D. Zollman, M.A. McDonough, R.M. Johnson, J. Spencer, A. Makena, M.I. Abboud, S. Cahill, S.Y. Lee, P.J. McHugh, C.J. Schofield, C.W.G. Fishwick, In Silico Fragment-Based Design Identifies Subfamily B1 Metallo- β -lactamase Inhibitors, *J. Med. Chem.* 61 (2018) 1255–1260. <https://doi.org/10.1021/acs.jmedchem.7b01728>.
- [8] F.-M. Klingler, D. Moser, D. Büttner, T.A. Wichelhaus, F. Löhr, V. Dötsch, E. Proschak, Probing metallo- β -lactamases with molecular fragments identified by consensus docking, *Bioorg. Med. Chem. Lett.* 25 (2015) 5243–5246. <https://doi.org/10.1016/j.bmcl.2015.09.056>.
- [9] T. Christopeit, A. Albert, H.-K.S. Leiros, Discovery of a novel covalent non- β -lactam inhibitor of the metallo- β -lactamase NDM-1, *Bioorg. Med. Chem.* 24 (2016) 2947–2953. <https://doi.org/10.1016/j.bmc.2016.04.064>.
- [10] R. Azumah, J. Dutta, A.M. Somboro, M. Ramtahal, L. Chonco, R. Parboosing, L.A. Bester, H.G. Kruger, T. Naicker, S.Y. Essack, T. Govender, In vitro evaluation of metal chelators as potential metallo- β -lactamase inhibitors, *J. Appl. Microbiol.* 120 (2016) 860–867. <https://doi.org/10.1111/jam.13085>.
- [11] Venatorx Pharmaceuticals, Inc., A Phase 3, Randomized, Double-blind, Active Controlled Noninferiority Study Evaluating the Efficacy, Safety, and Tolerability of Cefepime/VNRX-5133 in Adults With Complicated Urinary Tract Infections (cUTI), Including Acute Pyelonephritis, [clinicaltrials.gov](https://clinicaltrials.gov/ct2/show/NCT03840148), 2022. <https://clinicaltrials.gov/ct2/show/NCT03840148> (accessed March 12, 2023).
- [12] Qpex Biopharma, Inc., A Phase 1, Randomized, Double-Blind, Placebo-Controlled, Ascending Single and Multiple-Dose Study of the Safety, Tolerability and Pharmacokinetics of Intravenous (IV) QPX7728 Alone and in Combination With QPX2014 in Healthy Adult Subjects, [clinicaltrials.gov](https://clinicaltrials.gov/ct2/show/NCT04380207), 2022. <https://clinicaltrials.gov/ct2/show/NCT04380207> (accessed March 27, 2023).
- [13] D. Yong, M.A. Toleman, C.G. Giske, H.S. Cho, K. Sundman, K. Lee, T.R. Walsh, Characterization of a new metallo-beta-lactamase gene, bla(NDM-1), and a novel erythromycin esterase gene carried on a unique genetic structure in *Klebsiella pneumoniae* sequence type 14 from India, *Antimicrob. Agents Chemother.* 53 (2009) 5046–5054. <https://doi.org/10.1128/AAC.00774-09>.
- [14] K.K. Kumarasamy, M.A. Toleman, T.R. Walsh, J. Bagaria, F. Butt, R. Balakrishnan, U. Chaudhary, M. Doumith, C.G. Giske, S. Irfan, P. Krishnan, A.V. Kumar, S. Maharjan, S. Mushtaq, T. Noorie, D.L. Paterson, A. Pearson, C. Perry, R. Pike, B. Rao, U. Ray, J.B. Sarma, M. Sharma, E. Sheridan, M.A. Thirunarayan, J. Turton, S. Upadhyay, M. Warner, W. Welfare, D.M. Livermore, N. Woodford, Emergence of a new antibiotic resistance mechanism in India, Pakistan, and the UK: a molecular, biological, and epidemiological study, *Lancet Infect. Dis.* 10 (2010) 597–602. [https://doi.org/10.1016/S1473-3099\(10\)70143-2](https://doi.org/10.1016/S1473-3099(10)70143-2).
- [15] J. Brem, S.S. Van Berkel, W. Aik, A.M. Rydzik, M.B. Avison, I. Pettinati, K.-D. Umland, A. Kawamura, J. Spencer, T.D. Claridge, Rhodanine hydrolysis leads to potent thioenolate mediated metallo- β -lactamase inhibition, *Nat. Chem.* 6 (2014) 1084–1090.
- [16] B. Chandar, S. Poovitha, K. Ilango, R. MohanKumar, M. Parani, Inhibition of New Delhi Metallo- β -Lactamase 1 (NDM-1) Producing *Escherichia coli* IR-6 by Selected Plant Extracts and Their Synergistic Actions with Antibiotics, *Front. Microbiol.* 8 (2017). <https://doi.org/10.3389/fmicb.2017.01580>.
- [17] K. Koteva, A.M. King, A. Capretta, G.D. Wright, Total Synthesis and Activity of the Metallo- β -lactamase Inhibitor Aspergillomarasmine A, *Angew. Chem. Int. Ed.* 55 (2016) 2210–2212. <https://doi.org/10.1002/anie.201510057>.

- [18] W.B. Jin, C. Xu, Q. Cheng, X.L. Qi, W. Gao, Z. Zheng, E.W.C. Chan, Y.-C. Leung, T.H. Chan, K.-Y. Wong, S. Chen, K.-F. Chan, Investigation of synergistic antimicrobial effects of the drug combinations of meropenem and 1,2-benzisoxazol-3(2H)-one derivatives on carbapenem-resistant Enterobacteriaceae producing NDM-1, *Eur. J. Med. Chem.* 155 (2018) 285–302. <https://doi.org/10.1016/j.ejmech.2018.06.007>.
- [19] G. Rivière, S. Oueslati, M. Gayral, J.-B. Créchet, N. Nhiri, E. Jacquet, J.-C. Cintrat, F. Giraud, C. van Heijenoort, E. Lescop, S. Pethe, B.I. Iorga, T. Naas, E. Guittet, N. Morellet, NMR Characterization of the Influence of Zinc(II) Ions on the Structural and Dynamic Behavior of the New Delhi Metallo- β -Lactamase-1 and on the Binding with Flavonols as Inhibitors, *ACS Omega* 5 (2020) 10466–10480. <https://doi.org/10.1021/acsomega.0c00590>.
- [20] Y. Jia, B. Schroeder, Y. Pfeifer, C. Fröhlich, L. Deng, C. Arkona, B. Kuroпка, J. Sticht, K. Ataka, S. Bergemann, G. Wolber, C. Nitsche, M. Mielke, H.-K.S. Leiros, G. Werner, J. Rademann, Kinetics, Thermodynamics, and Structural Effects of Quinoline-2-Carboxylates, Zinc-Binding Inhibitors of New Delhi Metallo- β -lactamase-1 Re-sensitizing Multidrug-Resistant Bacteria for Carbapenems, *J. Med. Chem.* 66 (2023) 11761–11791. <https://doi.org/10.1021/acs.jmedchem.3c00171>.
- [21] J. Caburet, B. Boucherle, S. Bourdillon, G. Simoncelli, F. Verdirosa, J.-D. Docquier, Y. Moreau, I. Krimm, S. Crouzy, M. Peuchmaur, A fragment-based drug discovery strategy applied to the identification of NDM-1 β -lactamase inhibitors, *Eur. J. Med. Chem.* 240 (2022) 114599. <https://doi.org/10.1016/j.ejmech.2022.114599>.
- [22] J.C.J.M.D.S. Menezes, Arylidene indanone scaffold: medicinal chemistry and structure–activity relationship view, *RSC Adv.* 7 (2017) 9357–9372. <https://doi.org/10.1039/C6RA28613E>.
- [23] B. Boucherle, M. Peuchmaur, A. Boumendjel, R. Haudecoeur, Occurrences, biosynthesis and properties of aurones as high-end evolutionary products, *Phytochemistry* 142 (2017) 92–111. <https://doi.org/10.1016/j.phytochem.2017.06.017>.
- [24] I. Mazziotti, G. Petrarolo, C. La Motta, Aurones: A Golden Resource for Active Compounds, *Molecules* 27 (2022) 2. <https://doi.org/10.3390/molecules27010002>.
- [25] G. Sui, T. Li, B. Zhang, R. Wang, H. Hao, W. Zhou, Recent advances on synthesis and biological activities of aurones, *Bioorg. Med. Chem.* 29 (2021) 115895. <https://doi.org/10.1016/j.bmc.2020.115895>.
- [26] L.M. Lazinski, G. Royal, M. Robin, M. Maresca, R. Haudecoeur, Bioactive Aurones, Indanones, and Other Hemiindigoid Scaffolds: Medicinal Chemistry and Photopharmacology Perspectives, *J. Med. Chem.* 65 (2022) 12594–12625. <https://doi.org/10.1021/acs.jmedchem.2c01150>.
- [27] S. Okombi, D. Rival, S. Bonnet, A.-M. Mariotte, E. Perrier, A. Boumendjel, Discovery of Benzylidenebenzofuran-3(2H)-one (Aurones) as Inhibitors of Tyrosinase Derived from Human Melanocytes, *J. Med. Chem.* 49 (2006) 329–333. <https://doi.org/10.1021/jm050715i>.
- [28] S. Venkateswarlu, G.K. Panchagnula, G.V. Subbaraju, Synthesis and Antioxidative Activity of 3',4',6,7-Tetrahydroxyaurone, a Metabolite of *Bidens frondosa*, *Biosci. Biotechnol. Biochem.* 68 (2004) 2183–2185. <https://doi.org/10.1271/bbb.68.2183>.
- [29] A. Meguellati, A. Ahmed-Belkacem, W. Yi, R. Haudecoeur, M. Crouillère, R. Brillet, J.-M. Pawlotsky, A. Boumendjel, M. Peuchmaur, B-ring modified aurones as promising allosteric inhibitors of hepatitis C virus RNA-dependent RNA polymerase, *Eur. J. Med. Chem.* 80 (2014) 579–592. <https://doi.org/10.1016/j.ejmech.2014.04.005>.
- [30] A. Legru, F. Verdirosa, Y. Vo-Hoang, G. Tassone, F. Vascon, C.A. Thomas, F. Sannio, G. Corsica, M. Benvenuti, G. Feller, R. Coulon, F. Marcoccia, S.R. Devente, E. Bouajila, C. Piveteau, F. Leroux, R. Deprez-Poulain, B. Deprez, P. Licznar-Fajardo, M.W. Crowder, L. Cendron, C. Pozzi, S. Mangani, J.-D. Docquier, J.-F. Hernandez, L. Gavara, Optimization of 1,2,4-Triazole-3-thiones toward Broad-Spectrum Metallo- β -lactamase Inhibitors Showing Potent Synergistic Activity on VIM- and NDM-1-Producing Clinical Isolates, *J. Med. Chem.* 65 (2022) 16392–16419. <https://doi.org/10.1021/acs.jmedchem.2c01257>.

- [31] J.C. Hamrick, J.-D. Docquier, T. Uehara, C.L. Myers, D.A. Six, C.L. Chatwin, K.J. John, S.F. Vernacchio, S.M. Cusick, R.E.L. Trout, C. Pozzi, F. De Luca, M. Benvenuti, S. Mangani, B. Liu, R.W. Jackson, G. Moeck, L. Xerri, C.J. Burns, D.C. Pevear, D.M. Daigle, VNRX-5133 (Taniborbactam), a Broad-Spectrum Inhibitor of Serine- and Metallo- β -Lactamases, Restores Activity of Cefepime in Enterobacterales and *Pseudomonas aeruginosa*, *Antimicrob. Agents Chemother.* 64 (2020) 10.1128/aac.01963-19. <https://doi.org/10.1128/aac.01963-19>.
- [32] E. Boukherrouba, C. Larosa, K.-A. Nguyen, J. Caburet, L. Lunven, H. Bonnet, A. Fortuné, A. Boumendjel, B. Boucherle, S. Chierici, M. Peuchmaur, Exploring the structure-activity relationship of benzylidene-2,3-dihydro-1H-inden-1-one compared to benzofuran-3(2H)-one derivatives as inhibitors of tau amyloid fibers, *Eur. J. Med. Chem.* 231 (2022) 114139. <https://doi.org/10.1016/j.ejmech.2022.114139>.
- [33] R. Haudecoeur, A. Ahmed-Belkacem, W. Yi, A. Fortuné, R. Brillet, C. Belle, E. Nicolle, C. Pallier, J.-M. Pawlotsky, A. Boumendjel, Discovery of Naturally Occurring Aurones That Are Potent Allosteric Inhibitors of Hepatitis C Virus RNA-Dependent RNA Polymerase, *J. Med. Chem.* 54 (2011) 5395–5402. <https://doi.org/10.1021/jm200242p>.
- [34] R. Haudecoeur, A. Gouron, C. Dubois, H. Jamet, M. Lightbody, R. Hardré, A. Milet, E. Bergantino, L. Bubacco, C. Belle, M. Réglie, A. Boumendjel, Investigation of Binding-Site Homology between Mushroom and Bacterial Tyrosinases by Using Aurones as Effectors, *ChemBioChem.* 15 (2014) 1325–1333. <https://doi.org/10.1002/cbic.201402003>.
- [35] L. Lunven, H. Bonnet, S. Yahiaoui, W. Yi, L. Da Costa, M. Peuchmaur, A. Boumendjel, S. Chierici, Disruption of Fibers from the Tau Model AcPHF6 by Naturally Occurring Aurones and Synthetic Analogues, *ACS Chem. Neurosci.* 7 (2016) 995–1003. <https://doi.org/10.1021/acschemneuro.6b00102>.
- [36] C.-Y. Lee, E.-H. Chew, M.-L. Go, Functionalized aurones as inducers of NAD(P)H:quinone oxidoreductase 1 that activate AhR/XRE and Nrf2/ARE signaling pathways: Synthesis, evaluation and SAR, *Eur. J. Med. Chem.* 45 (2010) 2957–2971. <https://doi.org/10.1016/j.ejmech.2010.03.023>.
- [37] Y.H. Lee, M.C. Shin, Y.D. Yun, S.Y. Shin, J.M. Kim, J.M. Seo, N.-J. Kim, J.H. Ryu, Y.S. Lee, Synthesis of aminoalkyl-substituted aurone derivatives as acetylcholinesterase inhibitors, *Bioorg. Med. Chem.* 23 (2015) 231–240. <https://doi.org/10.1016/j.bmc.2014.11.004>.
- [38] H. Olleik, S. Yahiaoui, B. Roulier, E. Courvoisier-Dezord, J. Perrier, B. Pérès, A. Hijazi, E. Baydoun, J. Raymond, A. Boumendjel, M. Maresca, R. Haudecoeur, Aurone derivatives as promising antibacterial agents against resistant Gram-positive pathogens, *Eur. J. Med. Chem.* 165 (2019) 133–141. <https://doi.org/10.1016/j.ejmech.2019.01.022>.
- [39] B. Roulier, I. Rush, L.M. Lazinski, B. Pérès, H. Olleik, G. Royal, A. Fishman, M. Maresca, R. Haudecoeur, Resorcinol-based hemiindigoid derivatives as human tyrosinase inhibitors and melanogenesis suppressors in human melanoma cells, *Eur. J. Med. Chem.* 246 (2023) 114972. <https://doi.org/10.1016/j.ejmech.2022.114972>.
- [40] I. Hawkins, S.T. Handy, Synthesis of aurones under neutral conditions using a deep eutectic solvent, *Tetrahedron.* 69 (2013) 9200–9204. <https://doi.org/10.1016/j.tet.2013.08.060>.
- [41] S. Yahiaoui, M. Peuchmaur, A. Boumendjel, A straightforward conversion of aurones to 2-benzoylbenzofurans: transformation of one class of natural products into another, *Tetrahedron.* 67 (2011) 7703–7707. <https://doi.org/10.1016/j.tet.2011.08.011>.
- [42] A. Frank, N. Hamidi, F. Xue, Regioselective alkylation of 2,4-dihydroxybenzaldehydes and 2,4-dihydroxyacetophenones, *Tetrahedron Lett.* 95 (2022) 153755. <https://doi.org/10.1016/j.tetlet.2022.153755>.
- [43] M. Duflos, M.-R. Nourrisson, J. Brelet, J. Courant, G. LeBaut, N. Grimaud, J.-Y. Petit, N-Pyridinyl-indole-3-(alkyl) carboxamides and derivatives as potential systemic and topical inflammation inhibitors, *Eur. J. Med. Chem.* 36 (2001) 545–553.
- [44] M.J. Martin, B.W. Corey, F. Sannio, L.R. Hall, U. MacDonald, B.T. Jones, E.G. Mills, C. Harless, J. Stam, R. Maybank, Y. Kwak, K. Schaufler, K. Becker, N.-O. Hübner, S. Cresti, G. Tordini, M.

- Valassina, M.G. Cusi, J.W. Bennett, T.A. Russo, P.T. McGann, F. Lebreton, J.-D. Docquier, Anatomy of an extensively drug-resistant *Klebsiella pneumoniae* outbreak in Tuscany, Italy, Proc. Natl. Acad. Sci. 118 (2021) e2110227118. <https://doi.org/10.1073/pnas.2110227118>.
- [45] F. Cockerill, Methods for dilution antimicrobial susceptibility tests for bacteria that grow aerobically: approved standard, Tenth edition, Clinical and Laboratory Standards Institute, Wayne, Pa., 2015.
- [46] G.M. Morris, R. Huey, W. Lindstrom, M.F. Sanner, R.K. Belew, D.S. Goodsell, A.J. Olson, AutoDock4 and AutoDockTools4: Automated docking with selective receptor flexibility, J. Comput. Chem. 30 (2009) 2785–2791. <https://doi.org/10.1002/jcc.21256>.
- [47] D. Santos-Martins, S. Forli, M.J. Ramos, A.J. Olson, AutoDock4_{Zn} : An Improved AutoDock Force Field for Small-Molecule Docking to Zinc Metalloproteins, J. Chem. Inf. Model. 54 (2014) 2371–2379. <https://doi.org/10.1021/ci500209e>.
- [48] R. Dennington, Todd A. Keith, J.M. Millam, GaussView, (n.d.).
- [49] Schrödinger Suite Schrödinger, LLC, New York, NY., (2011).